

NASA Contractor Report 182284

# Computed Performance of the Half-Scale Accurate Antenna Reflector

Kevin M. Lambert  
*Analex Corporation*  
*NASA Lewis Research Center*  
*Cleveland, Ohio*

May 1989

Prepared for  
Lewis Research Center  
Under Contract NAS3-24564



National Aeronautics and  
Space Administration

(NASA-CR-182284) COMPUTED PERFORMANCE OF  
THE HALF-SCALE ACCURATE ANTENNA REFLECTOR  
Final Report (Analex Corp.) 33 p CSCL 09C

N 89-24532

Unclass

G 3/33 0217638

# COMPUTED PERFORMANCE OF THE HALF-SCALE ACCURATE ANTENNA REFLECTOR

Kevin M. Lambert  
Analex Corporation  
NASA Lewis Research Center  
Cleveland, Ohio 44135

## SUMMARY

This report studies the performance of the half scale, accurate antenna reflector (ref. 1). The antenna is evaluated for use as a compact range reflector. The reflector is studied for use with three separate feed antennas.

## INTRODUCTION

This report studies the computed performance of the half-scale, accurate antenna reflector (ref. 1). The goal is to evaluate the ability of the reflector to generate a near field, plane wave for a compact range application. The reflector is studied for use with an existing TRW dual mode horn feed, a proposed corrugated horn feed which provides a -20 dB edge illumination, and a corrugated waveguide feed which provides a -30 dB edge illumination.

## REFLECTOR GEOMETRY

The geometry of the half-scale accurate antenna reflector is as shown in figure 1. The reflector is a section of a paraboloid having a focal distance of 66 in. The bottom of the reflector is 28.06 in. above the axis of the generating paraboloid and the diameter of the reflector is 53.40 in. The reflector is obtained from the generating paraboloid in a manner such that the projection of the reflector onto any vertical plane is a 53.40 in. diameter circle. This is shown in figure 2.

The center of the circular aperture, when projected back to the reflector, defines the tilt angle which is required of the feed. The tilt angle locates the axis of the feed with respect to the axis of the paraboloid. This is shown in figure 3. For this antenna,

$$\text{Tilt Angle} = 45.063^\circ \quad . \quad (1)$$

With the axis of the feed defined, the angles subtended by the reflector, as viewed from the focal point, can be determined. In the vertical plane, let  $\theta_U$  represent the angle between the feed axis and the top of the reflector. Then,

$$\theta_U = 18.296^\circ \quad . \quad (2)$$

Similarly, let  $\theta_L$  represent the angle between the feed axis and the bottom of the reflector. Then,

$$\theta_L = 21.061^\circ \quad . \quad (3)$$

This information will be used later on when the aperture illumination of the reflector is discussed.

The angle subtended by the reflector, in the horizontal plane, may also be found. Let this angle be represented by  $\theta_s$ . Then,

$$\theta_s = 19.54^\circ \quad . \quad (4)$$

Note that since the reflector is symmetric about the  $y$  axis, this angle is representative of both the left and right side of the reflector.

#### TRW DUAL MODE HORN

Computed far field and near field patterns have been made for the reflector with the TRW dual mode horn as a feed. An accurate modeling of the electrical performance of the horn is dependent on the internal dimensions of the horn. These dimensions, obtained from TRW DWG #XC723795, are shown in figure 4.

The radiation patterns of this horn were computed for a frequency of 28.75 GHz, using the Ohio State University - Reflector Antenna Code (refs. 2 and 3). The patterns are computed in the standard spherical coordinate system with the aperture of the horn oriented as shown in figure 5. The heavy arrow in the aperture of the figure indicates that the electrical field polarization in the horn is in the  $y$  direction. Note that in this coordinate system a pattern with  $\phi = 0^\circ$  is the H-plane pattern of the horn and a pattern with  $\phi = 90^\circ$  is the E-plane pattern.

The H-plane pattern of the horn is shown in figure 6. Figure 6(a) is a plot of the magnitude and figure 6(b) is the phase. Note that only half of the pattern is shown because the pattern is symmetric with respect to  $\theta = 0^\circ$  (the  $z$  axis). The phase reference for the phase pattern is the coordinate origin which is in the aperture plane of the horn. The phase center of the horn can be found from this data through the use of the equation,

$$d = \frac{\alpha(\theta) - \alpha(0^\circ)}{[1 - \cos(\theta)]} \frac{\lambda}{360^\circ} \quad (5)$$

where  $\alpha(\theta)$  is the phase of the radiated field, in degrees, at the point  $\theta$ , and  $d$  is shown in figure 7.

Note  $d$  has the same units as  $\lambda$ . Using the H-plane data, the phase center is found to be,

$$d_H = 0.0649 \text{ in.} \quad (6)$$

where the subscript indicates that the phase center was found from H-plane data.

The magnitude of the field radiated in the E-plane of the horn is shown in figure 8(a). The phase is given in figure 8(b). Let  $d_E$  represent the phase center distance as calculated from E-plane data. Using the data in figure 8(b) and equation (5), this E-plane phase center can be found as,

$$d_E = 0.2414 \text{ in.} \quad (7)$$

Comparison of equations (6) and (7) shows that the H-plane and E-plane phase centers of the horn are not the same. In the calculated reflector patterns, which will be presented next, the actual phase center of the the horn is taken as the average of the two separate phase centers,

$$d = \frac{d_H + d_E}{2} = 0.153 \text{ in.}$$

The H-plane phase pattern, with the phase reference at this position, is shown in figure 9. Note that the phase is relatively flat over the region which will be illuminating the reflector ( $\theta \leq 20^\circ$ ). The E-plane phase pattern, with the phase reference adjusted to the phase center, is given in figure 10. This phase pattern has also flattened out, however it falls off more quickly than the H-plane. This is because the main beam in the E-plane is narrower than the main beam in the H-plane.

#### FAR FIELD PATTERNS OF THE REFLECTOR ANTENNA

The feed patterns, given in the previous section, are used with the reflector geometry, discussed in the first section, to generate the patterns of the reflector antenna. The coordinate system used for the patterns is shown in figure 11. A nonstandard spherical coordinate system is used. Although  $\phi$  is still defined as the angle from the x axis of the projection of the radial vector, onto the x-y plane, the following is used

$$-90^\circ \leq \phi \leq 90^\circ$$

$$-180^\circ \leq \theta \leq 180^\circ$$

Additionally, the x axis will be assumed to be the horizontal direction and the y axis will be the vertical. Figures 12 and 13 show the H-plane and E-plane patterns of the reflector antenna for the feed horizontally polarized. Again, the patterns were calculated using the Ohio State University - Reflector Antenna Code. Figures 14 and 15 show the H-plane and the E-plane patterns for the feed, vertically polarized.

A major characteristic of the orientation of the feed is the location of the feed spillover lobes. For example, the large lobe at  $75^\circ$  in figure 15(b) is due to spillover of the sidelobe at  $67^\circ$  in the feed pattern shown in figure 8(a). When the feed is rotated, from vertical polarization to horizontal polarization, this spillover lobe rotates to the other plane. Therefore, the lobe does not appear in figure 12(b).

#### NEAR FIELD PATTERNS OF THE REFLECTOR ANTENNA

The near field patterns of the reflector antenna may also be computed. They are computed using the coordinate system shown in figure 16. Note that this is a cylindrical coordinate system centered on the aperture.

The range, or distance from the vertex of the reflector to the scan plane, of the patterns is  $z = 132$  in. as shown in figure 17.

As in the far field calculations, the  $x$  direction is the horizontal direction. However, data will only be shown for the feed horizontally polarized.

Figure 18 shows the magnitude and phase patterns for  $\theta = 90^\circ$  and  $-30 \text{ in.} \leq \rho \leq 30 \text{ in.}$ . Note that this is a vertical scan. Also recall that the reflector has a diameter of 53.40 in. Therefore,

$$-26.70 \text{ in.} \leq \rho \leq 26.70 \text{ in.}$$

is the projected aperture of the reflector in the scan plane.

Figure 19 displays the computed near field magnitude and phase for a horizontal scan. Again, the projected aperture is given by

$$-26.70 \text{ in.} \leq \rho \leq 26.70 \text{ in.}$$

Note that the horizontal scan is symmetric with respect to  $\rho = 0$ .

#### EVALUATION OF THE PERFORMANCE OF THE ANTENNA

The major goal of this study is to evaluate the ability of the antenna system to generate a near field plane wave for a compact range application. This section will discuss the antenna performance as it relates to this application.

A compact range is a measurement facility used for the testing of the far-field response of antennas and scatterers. The compact range has an advantage over conventional farfield ranges in that the testing takes place in a smaller volume. For example, a Scientific Atlanta, Model 5751 compact range can measure a 4 ft diameter antenna, at 18 GHz in a 17 by 20 by 36 ft room. To measure the same antenna in a farfield range would require a minimum separation between source and receiver of  $586 \text{ ft}$  ( $2D^2/\lambda$ ).

A compact range achieves this savings in space by performing the testing in the near field of a parabolic reflector antenna. This is possible because a component of the near field response of the reflector is a plane wave. Ideally, a compact range would operate as shown in figure 20.

A point source feed, emanating a spherical wave, would be placed at the focus of the parabolic reflector. The energy in the spherical wave is collimated by the properties of the reflector and a uniform plane wave is produced. The object to be tested is placed in this plane wave field as shown in figure 21. In this manner, the response of the object to an incident plane wave can be measured. The volume in which the compact range reflector generates a plane wave is called the quiet zone.

In practice, the ideal compact range cannot be realized and can only be approximated. There are numerous reasons for why this is true, however only the reasons which pertain to the compact range feed/reflector system will be described. This will allow the characteristics of the half-scale antenna to be discussed in relation to the compact range application.

In the practical compact range, there are several factors which act to corrupt the plane wave generated by the compact range reflector. These factors affect the quality of the quiet zone and limit the accuracy of the measurements. Begin with the reflector feed. Practical feeds cannot produce a spherical wave of uniform amplitude and phase. Instead they produce magnitude and phase responses that are a function of angle. This was seen for the TRW feed in the patterns given in section II. Such a feed pattern introduces amplitude and phase taper in the quiet zone. This is demonstrated in figure 22.

As shown in figure 22 a plane wave is no longer being generated. The original quiet zone, shown by A-A', must now be reduced in size, to a region where the wave is still nearly plane. This is shown by B-B' in the figure. Generally, the size of B-B' is taken as the region where no more than 1 dB of amplitude taper exists. Within this region, there should be no more than 22.5° of phase taper (the same as the farfield criteria). Thus, the characteristics of the feed radiation pattern control the size of the quiet zone (for a given reflector). In general, the more directive the feed, the smaller the quiet zone. Since all antennas have some directivity, the quiet zone is always smaller than the projected aperture of the reflector.

Thus far, the discussion has just been concerned with the field reflected by the compact range antenna. This field is also known as the geometrical optics field because it is the field which obeys Snell's Law at the reflector surface. This field is the field which is desired in the quiet zone. However, there are other, undesirable fields in the quiet zone. The two which are associated with the compact range antenna system are shown in figure 23.

These fields are the spillover energy of the feed, which is directed toward the quiet zone, and the fields diffracted from the edge of the reflector, toward the quiet zone. These fields affect the quality of the quiet zone by introducing an amplitude and phase ripple into the total field. The total field may be written as,

$$\bar{E}^T = \bar{E}^{G.O.} + \bar{E}^D + \bar{E}^F$$

The ripple occurs as the individual terms add in and out of phase. The goal in the design of modern compact ranges is to prevent the ripple from being greater than 0.1 dB. A great deal of research is being conducted in order to obtain designs that achieve this goal. Techniques include: reflector edge treatments, feed pattern/aperture distribution control, and isolation of the feed from the quiet zone.

There are other factors which can corrupt the quality of the field in the quiet zone. However these are associated with interactions between the compact range antenna and the room in which the measurement takes place. These effects are not being considered in this study.

The half-scale antenna can now be evaluated in terms of a compact range application. The computed results given in this section are for the half-scale reflector with the TRW feed.

First, the geometrical optics field must be examined in order to define the quiet zone in terms of taper. Figure 24 shows the G.O. field in the

horizontal plane for the horizontally polarized feed. As would be expected, there is no field outside of the projected aperture of the reflector. Figure 25 is the same curve on an expanded scale and normalized. From this curve it can be seen that the quiet zone would be defined as

$$-8.50 \text{ in.} \leq \rho \leq 8.50 \text{ in.}, \quad \phi = 0^\circ \quad (9)$$

in the horizontal plane, on the basis of the 1 dB amplitude taper. From the G.O. phase plot, which is given in figure 26, it can be seen that the  $22.5^\circ$  phase taper criterion is easily met over the region indicated by equation 9.

The magnitude of the G.O. field in the vertical plane is shown in figure 27 and on an expanded scale in figure 28. The expanded scale plot indicates that the quiet zone would be defined as

$$-11.75 \leq \rho \leq 7.75, \quad \phi = 90^\circ \quad (10)$$

according to the 1 dB criterion. Examination of the phase plot in figure 29 shows that the phase taper criterion is adequate over this region as well.

In summary, it appears that the antenna produces a quiet zone that is approximately elliptic in cross-section. However, the ripple level must be examined in order to determine the quality of the quiet zone.

The total field in the quiet zone is given in the near field patterns that were presented in section IV. The ripple level could be determined from those patterns, however, it is instructive to examine the two field components which cause the ripple. Figure 30 shows the magnitude of the diffracted field in the horizontal plane. Note that in the center of the previously defined quiet zone, the diffracted field is on the order of 5 dB. Examination of figure 24 shows that the desired G.O. field is on the order of 21 dB there.

Thus, the diffracted field is only -16 dB relative to the G.O. field. To see what this means in terms of quiet zone ripple, assume that the two fields are in phase. Then, if

$$E_{G.O.} = 1 \text{ V}$$

and since the diffracted field is -16 dB relative,

$$E^D = 0.156 \text{ V}$$

then the combination produces (assuming spillover is insignificant for now)

$$E^t = E_{G.O.} + E^D = 1.156 \text{ V}$$

or

$$E^t = 1.26 \text{ dB} .$$

If the two are out of phase, then

$$E^t = 0.8440$$

or

$$E^t = -1.47 \text{ dB}$$

Thus, this diffracted field can be expected to produce at least, 2.73 dB peak to peak ripple in the quiet zone. This is a lot greater than the 0.1 dB ripple which is desired. Note that to achieve the 0.1 dB ripple, the diffracted field must be -40 dB relative to the G.O. field. For completeness, the phase of the diffracted field in the horizontal plane is shown in figure 31.

The magnitude of the diffracted field in the vertical plane is shown in figure 32. The phase is given in figure 33. In this plane, the diffracted field has a level which is only about -6 dB relative to the G.O. field. This level occurs only at one point in the quiet zone, however, it could cause the ripple to be on the order of several dB.

The final component of the total field, the feed spillover, is shown in figures 34 to 37. Figures 34 and 35 show the magnitude and phase of this component in the horizontal plane. Figures 36 and 37 show the magnitude and phase in the vertical plane. The spillover field is on the order of -50 dB relative to the G.O. field. Thus, it could be expected to generate ripple levels less than a tenth of a dB.

The actual ripple level depends on how the three individual components, which are phasors, combine. As mentioned earlier, the information is contained in the total near field plots which were given in section IV. The actual ripple level is difficult to determine from these plots because the ripple is super-imposed upon the taper of the G.O. field. To obtain the ripple level, the G.O. field can be subtracted from the total field. Mathematically, this gives,

$$\bar{E}^t - \bar{E}^{G.O.} = \bar{E}^D + \bar{E}^F$$

Figure 38 presents this field for the horizontal plane. From this figure, it can be determined that the ripple in the quiet zone ( $|\rho| \leq 8.50$  in.) is on the order of  $\pm 0.3$  dB.

Figure 39 presents the ripple for the vertical plane. From this figure, it can be determined that the ripple in the quiet zone is on the order of  $\pm 0.6$  dB.

Clearly the half-scale antenna with the TRW feed does not produce an acceptable quiet zone. Typically, compact ranges claim to use a quiet zone which has a cross section which 25 percent of the area of the projected aperture. The antenna being studied here produces a zone which is only 11 percent of the projected aperture. Thus, the antenna is not as efficient in producing a quiet zone as some designs. This reduction in the quiet zone imposes the limit on the size of the objects that can be measured. However, given the size of the quiet zone, the ripple caused by the diffracted field and the spillover field corrupts the quiet zone so much that it is doubtful that accurate microwave measurements can be performed. The problem is now to determine what can be done with this antenna system in order that accurate measurements can be performed. This subject will be discussed in the next section.

#### ANTENNA MODIFICATIONS FOR USE IN A COMPACT RANGE

The previous sections have presented the radiation characteristics of the half-scale accurate antenna reflector when used with the TRW dual mode horn

feed. This antenna was also evaluated with respect to an application as a compact range antenna system. This evaluation concluded that the performance of the antenna was unacceptable in that application. This section will investigate what might be done in order to achieve acceptable performance out of the reflector.

The half-scale reflector with the TRW horn was judged unacceptable for two reasons. First, the quiet zone, as defined by the 1 dB taper, is smaller than what is generally produced in commercial compact ranges. Second, the ripple levels in the quiet zone are unacceptable. To achieve better performance from the half-scale reflector, both of these issues must be addressed.

The size of the quiet zone is determined by the radiation pattern of the feed and the geometry of the reflector system. In the approximate sense, the size of the quiet zone is determined by the 1 dB beamwidth of the feed. This beamwidth is projected into the nearfield of the reflector as shown in figure 40. This relationship is exactly true for reflectors which have large F/D ratios. For reflectors with smaller F/D ratios, the varying distance between the focus and points on the reflector surface introduce an additional taper. This additional taper is called the space taper and it is shown plotted in figure 41 (ref. 4). The combination of feed distribution and space taper produce the aperture distribution for the reflector antenna which actually determines the size of the quiet zone.

Unfortunately, a feed pattern cannot be broadened to increase the size of the quiet zone without affecting the ripple in the quiet zone. Recall that the ripple is produced by the diffracted field from the edges of the reflector and the feed spillover. The magnitude of the diffracted field is directly related to the magnitude of the field incident upon the reflector edge. Thus, if the feed pattern is broadened to increase the quiet zone size, then it is likely that the ripple will increase due to the higher edge illumination of the reflector. Additionally, a feed which generates a broad feed pattern will also produce higher spillover levels. Thus, for a conventional reflector, there are trade offs to consider between quiet zone size and quality.

Currently, a great deal of discussion and research is directed toward minimizing the impact of these trade offs. Manufacturers and researchers have proposed various reflector edge treatments in order to reduce the diffracted field without giving up too much on the incident field. Also, absorber enclosures, walls and even separate rooms are being used to prevent direct feed energy from causing ripple in the target zone.

The modifications which can be applied to improve the performance of the half-scale reflector for a compact range application are limited. Obviously, the reflector already exists and has a fixed F/D ratio. Thus, the space taper is known and cannot be modified. The reflector has a conventional edge and so diffracted field reduction must come about through reduction of the incident field. Therefore the use of this reflector will depend on the quiet zone that remains once the edge illumination is brought down far enough to produce an acceptable ripple. Reduction of the edge illumination will require a feed which is more directive than the TRW feed. Since the TRW feed did not prove to have a substantial spillover level, the more directive feed is likely to have acceptable levels. Thus, this work will concentrate on finding an edge illumination which will provide the desired result.

Fortunately, the reflector is only required to produce a quiet zone which is at least 11 in. in diameter. This requirement comes from the size of the objects which will be measured. Therefore it will not be necessary to obtain the largest possible quiet zone. The size of the quiet zone can be reduced in order to obtain acceptable ripple levels.

Before examination of quiet zones resulting from lower edge illumination, it is instructive to determine what the edge illumination is with the TRW feed. The TRW feed had a tilt angle of 45.06° relative to the axis of the reflector. This tilt angle defines the axis of the feed and it is the direction of the main beam of the feed radiation pattern. The top edge of the reflector is 18.296° from the feed axis as shown in figure 42.

The top edge of the reflector is in the H-plane of the horizontally polarized feed. Thus, using figure 6, the feed pattern is found to be -6.17 dB. The additional space attenuation is found from figure 41. Radiation directed at the top edge of the reflector experiences an additional 1.42 dB attenuation over radiation directed at the center of the reflector. Thus, the top edge illumination is,

$$E_{TOP} = -6.17 \text{ dB} - 1.42 \text{ dB} = -7.59 \text{ dB}$$

relative to the center.

This same procedure can be applied to the bottom edge and to the sides as well. In summary,

$$E_{BOTTOM} = -7.30 \text{ dB}$$

and

$$E_{SIDES} = -10.70 \text{ dB}$$

Thus the edge illumination is approximately -7.5 dB in the vertical plane and -10.7 dB in the horizontal plane. The higher edge illumination in the vertical plane results in more ripple in that plane. This can be seen by comparing figures 38 and 39. Since -10.7 dB edge illumination produced an unacceptable ripple, lower illuminations will be investigated.

The first edge illumination to be tried is one that is approximately -20 dB with respect to the center of the aperture. Figure 43 shows the far-field pattern of a corrugated horn which will provide that illumination. The pattern of the horn is symmetric about the  $\theta = 0^\circ$  axis and it is also circularly symmetric. Thus, the H-plane and E-plane patterns are equal. This field pattern provides the following edge illuminations.

$$E_{TOP} = -19.61 \text{ dB}$$

$$E_{BOTTOM} = -20.40 \text{ dB}$$

$$E_{SIDES} = -20.39 \text{ dB}$$

The resulting near field pattern in the horizontal plane, at  $z = 132$  in. is shown in figure 44. Both the ripple and the quiet zone are noticeably reduced from those seen with the TRW horn. The near field pattern in the vertical plane is given in figure 45.

To determine the size of the quiet zone for this edge illumination, the G.O. fields are given. Figures 46 and 47 show the magnitude of the G.O. field in the horizontal plane. From figure 47, the 1 dB taper quiet zone is defined by  $|\rho| \leq 6$  in. This exceeds the 11 in. required. For completeness, the G.O. phase in the horizontal plane is given in figure 48. The magnitude of the G.O. field in the vertical plane is given in figures 49 and 50. These figures show that the quiet zone is given by

$$-6.75 \text{ in.} \leq \rho \leq 5.25 \text{ in.}$$

in the vertical plane. This also exceeds the 11 in. required and thus the -20 dB edge illumination provides a quiet zone of adequate size. The phase of the G.O. field in the vertical plane is given in figure 51.

The ripple in the quiet zone can again be determined by subtracting the G.O. field from the total field. Figure 52 shows the ripple in the horizontal plane. This figure shows that the ripple is almost acceptable, being on the order of  $\pm 0.1$  dB except at the center. The large spike at the center occurs because it lies along the caustic of the edge diffracted rays. Figure 53 shows similar performance in the vertical plane.

To further reduce the diffracted field, a lower edge illumination will be considered. A corrugated waveguide with a 2.176 in. internal diameter will radiate the pattern shown in figure 54. This pattern is circularly symmetric. Note that the first null in the pattern is located in the vicinity of the edges of the reflector. In fact, the edge illumination for this waveguide as a feed is

$$E_{TOP} = -33.5 \text{ dB}$$

$$E_{BOTTOM} = -30.4 \text{ dB}$$

$$E_{SIDES} = -50.5 \text{ dB}$$

relative to the radiation at the center.

The resulting near field pattern in the horizontal plane, at  $z = 132$  in. is shown in figure 55. Note that the quiet zone is again smaller and the ripple is almost imperceptable. The near field pattern in the vertical plane is given in figure 56.

The size of the quiet zone is determined by examining the G.O. field in the horizontal and vertical planes. Figures 57 and 58 show the magnitude of the G.O. field in the horizontal plane. Figure 59 is the phase. Again using the 1 dB taper criterion, the quiet zone in the horizontal plane is defined by

$$|\rho| \leq 5.5 \text{ in.}$$

which is just enough to accommodate the 11 in. test object. The magnitude of the G.O. field in the vertical plane is given in figures 60 and 61. The phase is given in figure 62. The quiet zone in this plane is defined by

$$-6.25 \text{ in.} \leq \rho \leq 5.00 \text{ in.}$$

which will also accommodate the 11 in. object.

The ripple in the horizontal plane of the quiet zone is provided in figure 63. Here it can be seen that an acceptable ripple level has been achieved. The ripple in the vertical plane is given in figure 64. This ripple is slightly larger than desired but it is probably acceptable.

#### SUMMARY AND CONCLUSIONS

Some calculated characteristics of the half-scale accurate antenna reflector have been presented. These characteristics have been used to evaluate the reflector for use in a compact range measurement facility. The baseline for the evaluation was taken to be a quiet zone with no more than 1 dB of amplitude taper and no more than 22.5° of phase taper. The quiet zone also had to have an amplitude ripple of no more than 0.1 dB.

The major difficulty in achieving the required quiet zone was shown to be the field diffracted from the edges of the reflector. Without modifying the edges mechanically, the only way to reduce the diffracted field was shown to be a very low edge illumination. The computed results showed that the edge illumination had to be on the order of -30 dB or lower in order to achieve acceptable ripple performance.

Lower ripple levels, by lowering the edge illumination, comes at a cost of a smaller quiet zone. With the -30 dB edge illumination, the cross section of the quiet zone contains only about 4 percent of the projected aperture of the reflector. However, this area is big enough to measure the test objects which are being contemplated.

This study did not consider the physical realization of the feed which would produce the -30 dB edge illumination. Such a feed could probably be designed at a given frequency. However, the feed would have a frequency response and the desired pattern might not be achieved at all frequencies. This could result in some frequencies where the quality of the quiet zone is unacceptable if swept frequency measurements are used.

Also, the effects of the room were not considered. Direct feed illumination of objects in the room will cause those objects to scatter energy into the quiet zone. This scattered energy will contribute to the ripple. Therefore it is possible that the quiet zone ripple would be unacceptable even with the ideal feed for the reflector.

In conclusion, the results presented here have shown that the half-scale reflector can be used for the compact range measurements being considered.

#### REFERENCES

1. NASA Drawing Numbers: 72076M40A000, 62076M40A100
2. W.D. Burnside, R.C. Rudduck and R.J. Marhefka, "Summary of GTD Computer Codes Developed at the Ohio State University," IEEE Trans. Electromagn. Compat., vol. EMC-22, no. 4, Nov. 1980

3. S.H. Lee and R.C. Rudduck, "Aperture Integration and GTD Techniques Used in the NEC Reflector Antenna Code." IEEE Trans. Antennas and Propagation, vol. AP-33, pp. 189-194, Feb. 1986
4. Richard C. Johnson, Henry Jasik, ed.; Antenna Engineering Handbook, 2nd edition McGraw Hill, New York, 1984, figures 17 to 19.

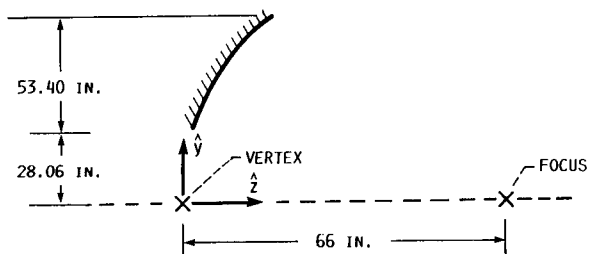


FIGURE 1. - SIDE VIEW OF THE HALF SCALE ACCURATE ANTENNA REFLECTOR.

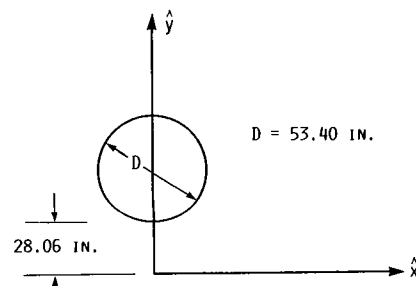


FIGURE 2. - PROJECTION OF THE HALF SCALE ACCURATE ANTENNA REFLECTOR ONTO AN ARBITRARY APERTURE PLANE.

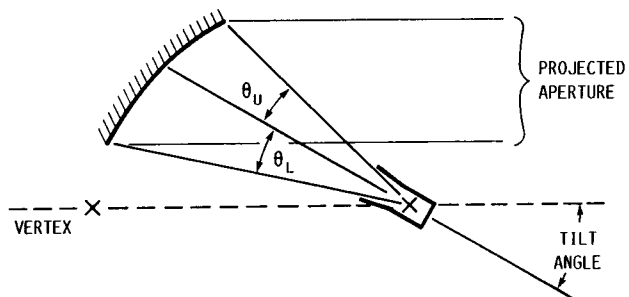


FIGURE 3. - TILT ANGLE AND SUBTENDED ANGLE FOR THE HALF SCALE ACCURATE ANTENNA REFLECTOR.

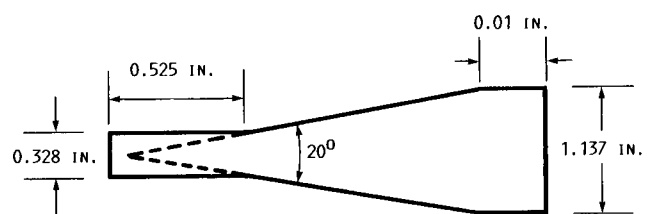


FIGURE 4. - INTERNAL DIMENSIONS OF THE TRW DUAL MODE HORN.

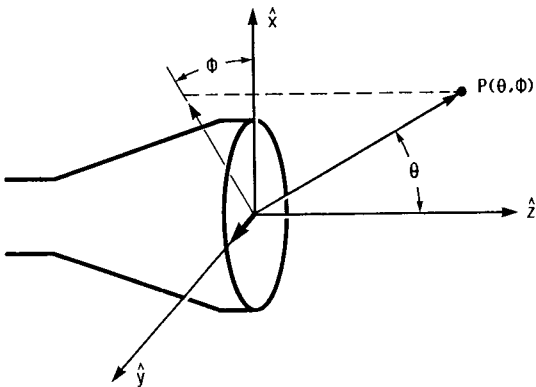


FIGURE 5. - COORDINATE SYSTEM FOR FARFIELD PATTERNS.

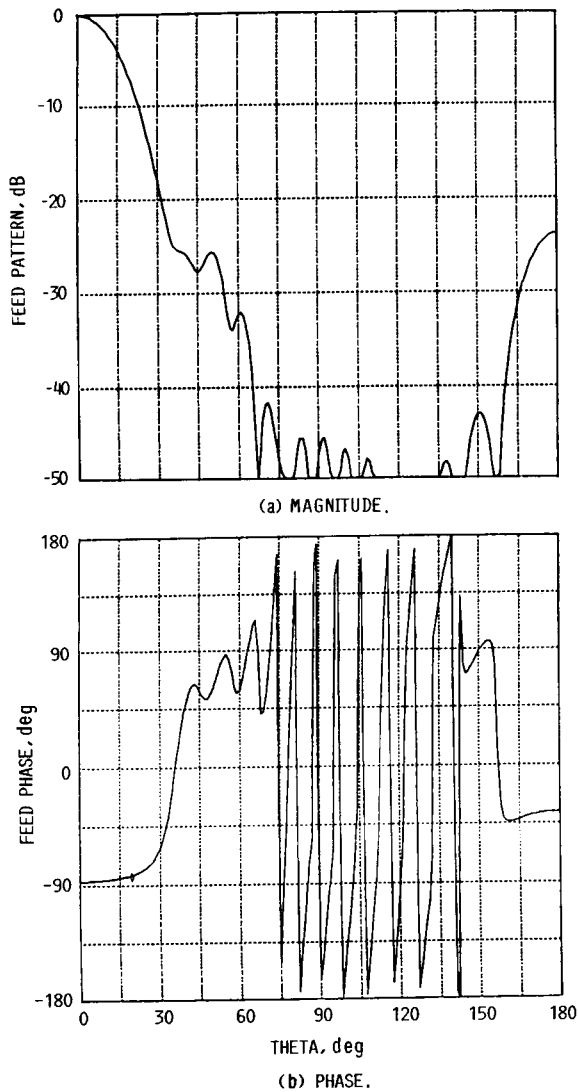


FIGURE 6. - CALCULATED H-PLANE PATTERN OF THE TRW DUAL MODE HORN,  $f = 28.75$  GHz.

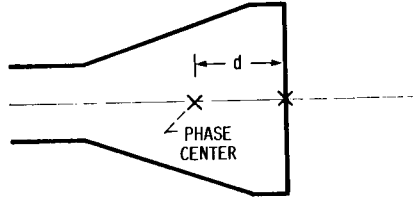


FIGURE 7. - PHASE CENTER RELATIONSHIP TO APERTURE PLANE.

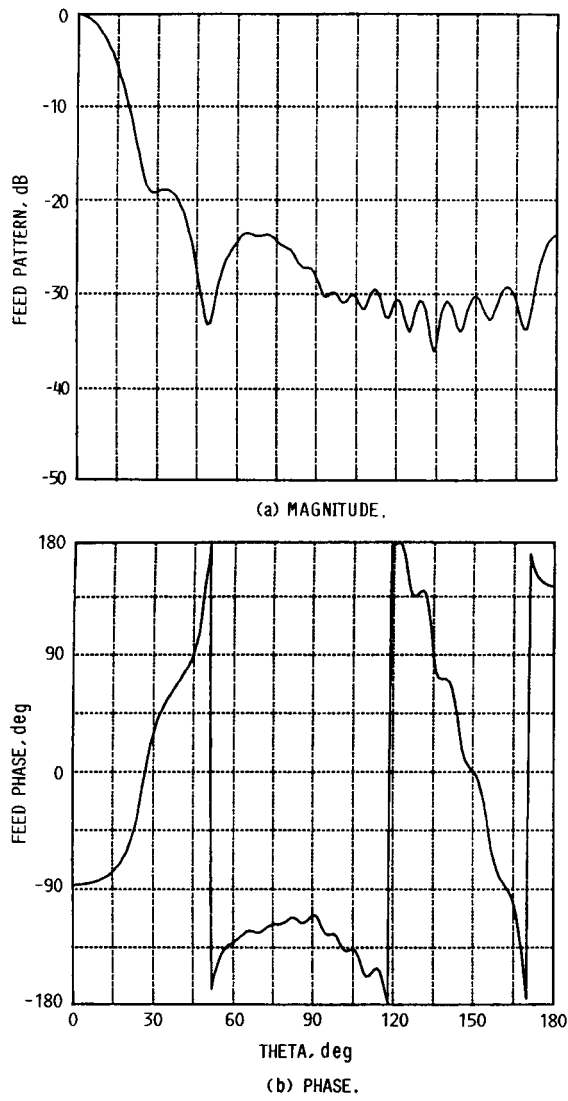


FIGURE 8. - CALCULATED E-PLANE PATTERN OF THE TRW DUAL MODE HORN,  $f = 28.75$  GHz.

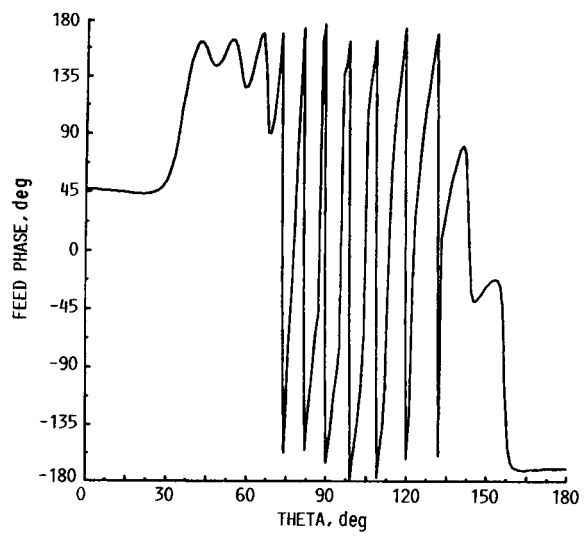


FIGURE 9. - H-PLANE PHASE PATTERN OF THE TRW DUAL MODE HORN WITH THE PLANE REFERENCE AT THE PHASE CENTER,  $d = 0.153$  IN.  $f = 28.75$  GHz.

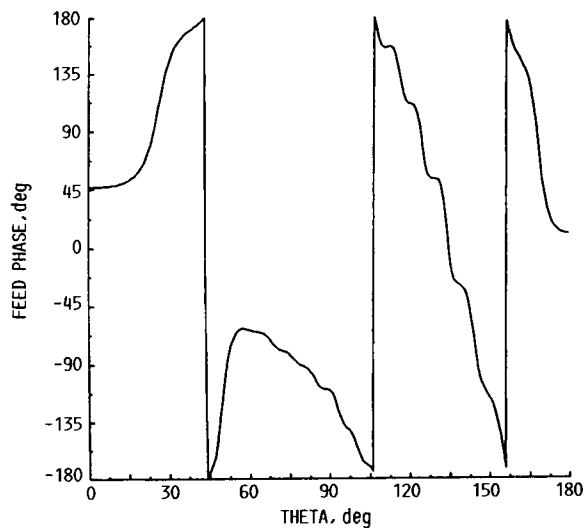


FIGURE 10. - E-PLANE PHASE PATTERN OF THE TRW DUAL MODE HORN WITH THE PHASE REFERENCE AT THE PHASE CENTER,  $d = 0.153$  IN.  $f = 28.75$  GHZ.

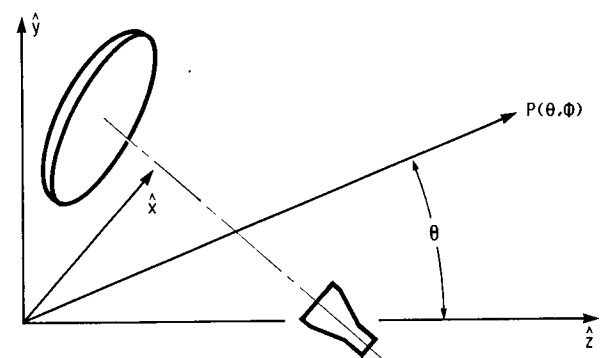


FIGURE 11. - COORDINATE SYSTEM FOR REFLECTOR FARFIELD PATTERNS.

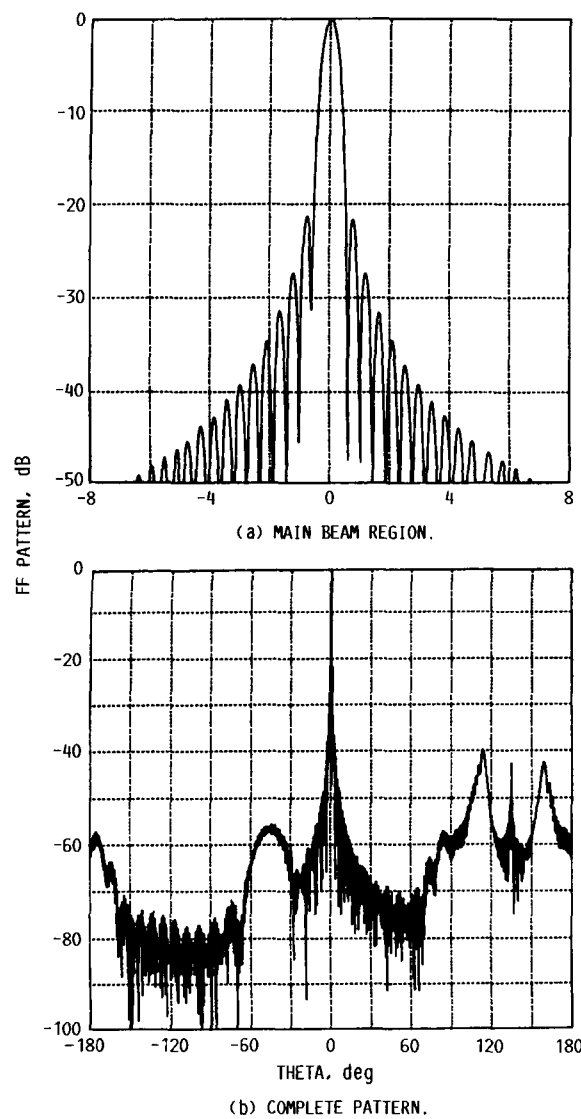


FIGURE 12. - CALCULATED H-PLANE PATTERN OF THE HALF SCALE ACCURATE ANTENNA REFLECTOR WITH THE TRW DUAL MODE HORN FEED. HORIZONTAL POLARIZATION,  $f = 28.75$  GHz.

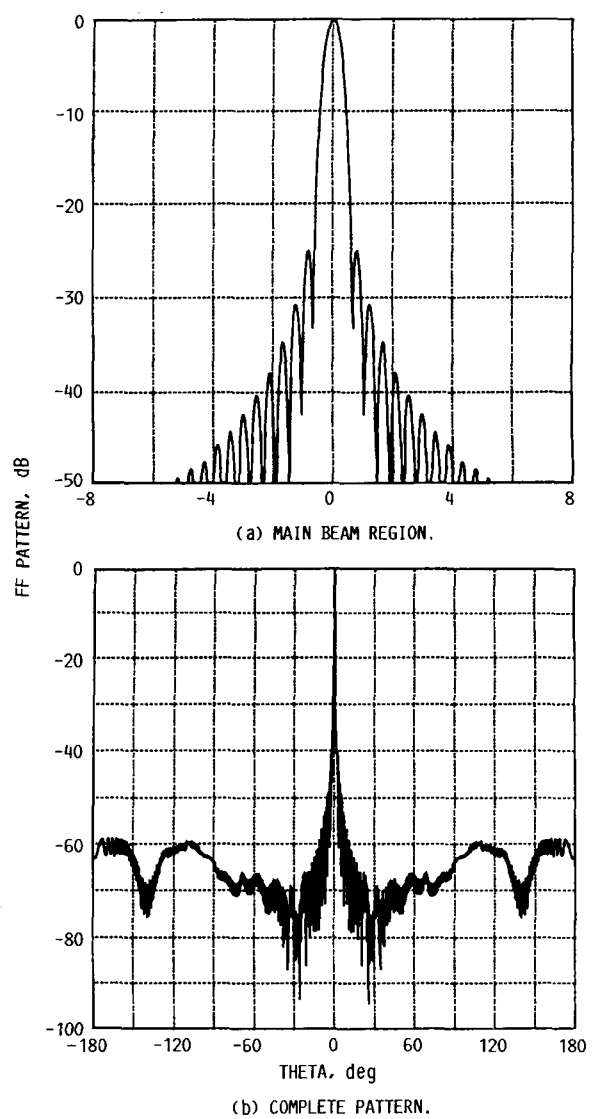
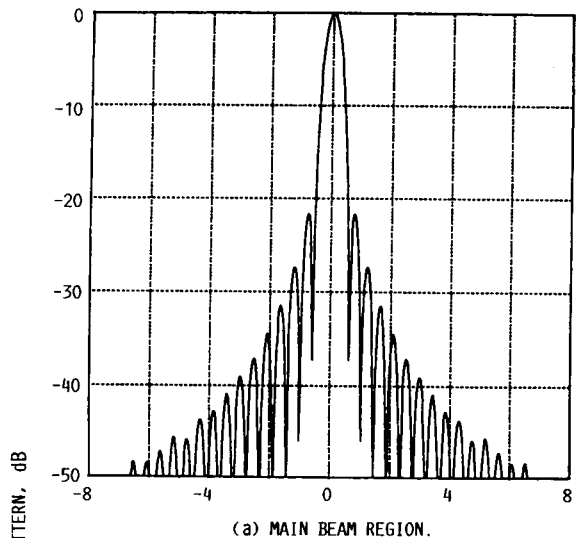
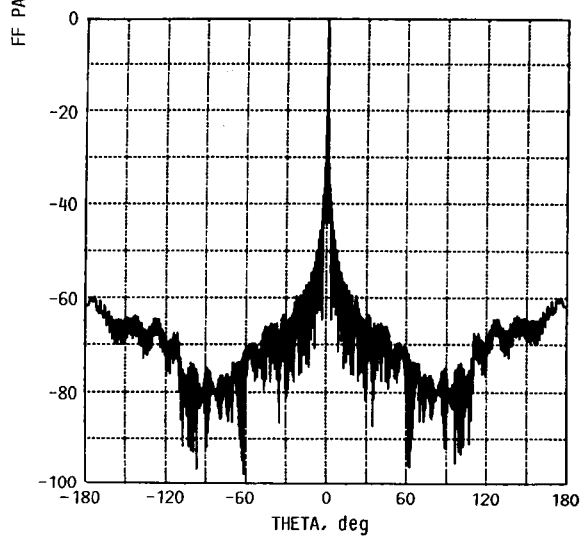


FIGURE 13. - CALCULATED E-PLANE PATTERN OF THE HALF SCALE ACCURATE ANTENNA REFLECTOR WITH THE TRW DUAL MODE HORN FEED. HORIZONTAL POLARIZATION,  $f = 28.75$  GHz.

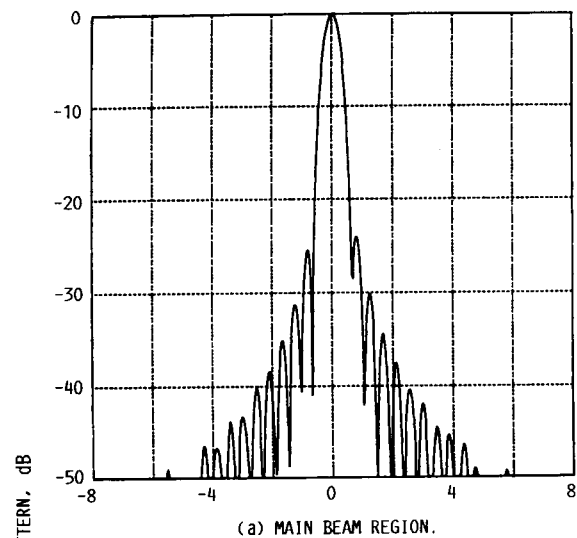


(a) MAIN BEAM REGION.

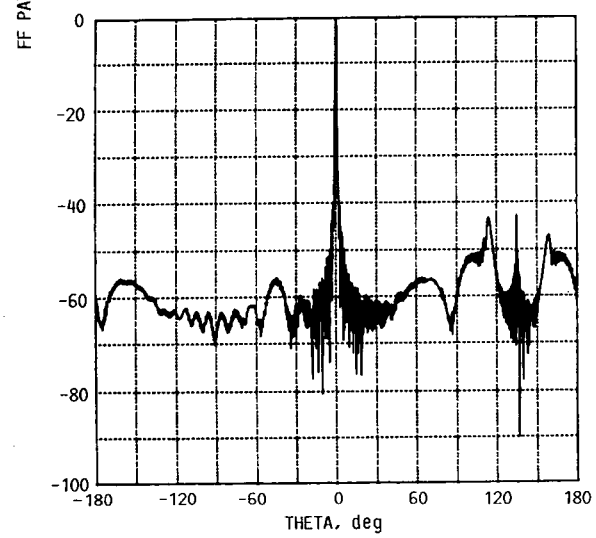


(b) COMPLETE PATTERN.

FIGURE 14. - CALCULATED H-PLANE PATTERN OF THE HALF SCALE ACCURATE ANTENNA REFLECTOR WITH THE TRW DUAL MODE HORN FEED. VERTICAL POLARIZATION,  $f = 28.75$  GHz.



(a) MAIN BEAM REGION.



(b) COMPLETE PATTERN.

FIGURE 15. - CALCULATED E-PLANE PATTERN OF THE HALF SCALE ACCURATE ANTENNA REFLECTOR WITH THE TRW DUAL MODE HORN FEED. VERTICAL POLARIZATION,  $f = 28.75$  GHz.

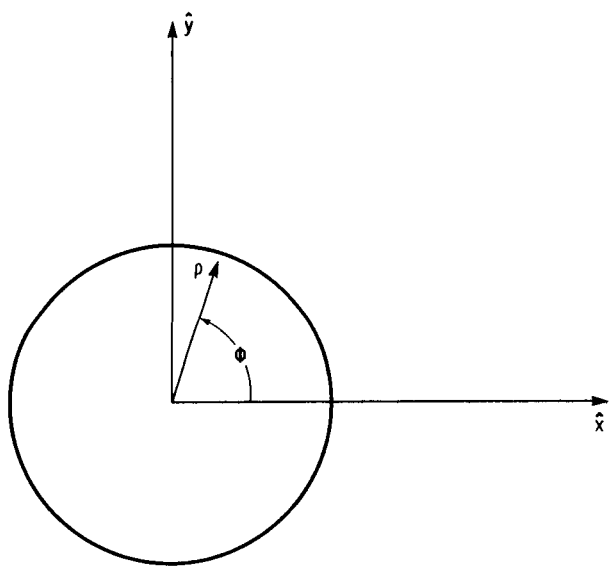


FIGURE 16. - COORDINATE SYSTEM FOR NEAR FIELD PATTERNS.

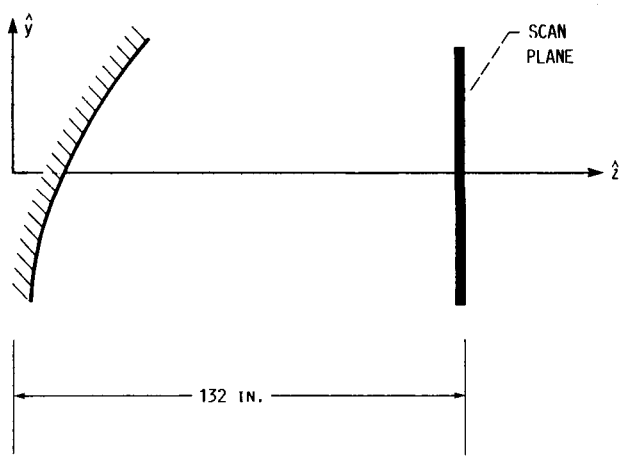


FIGURE 17. - THE RANGE USED IN THE NEAR FIELD CALCULATIONS.

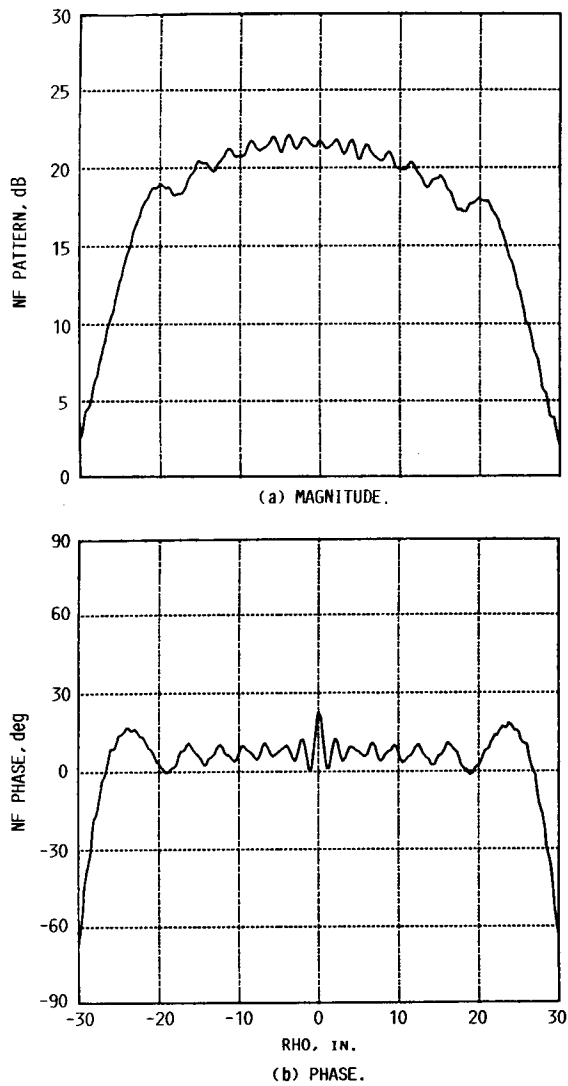


FIGURE 18. - VERTICAL SCAN OF THE NEAR FIELD AT  
 $z = 132$  IN. HALF SIZE ACCURATE ANTENNA REFLECTOR  
 WITH THE TRW DUAL MODE HORN. HORIZONTAL POLAR-  
 IZATION,  $f = 28.75$  GHZ.

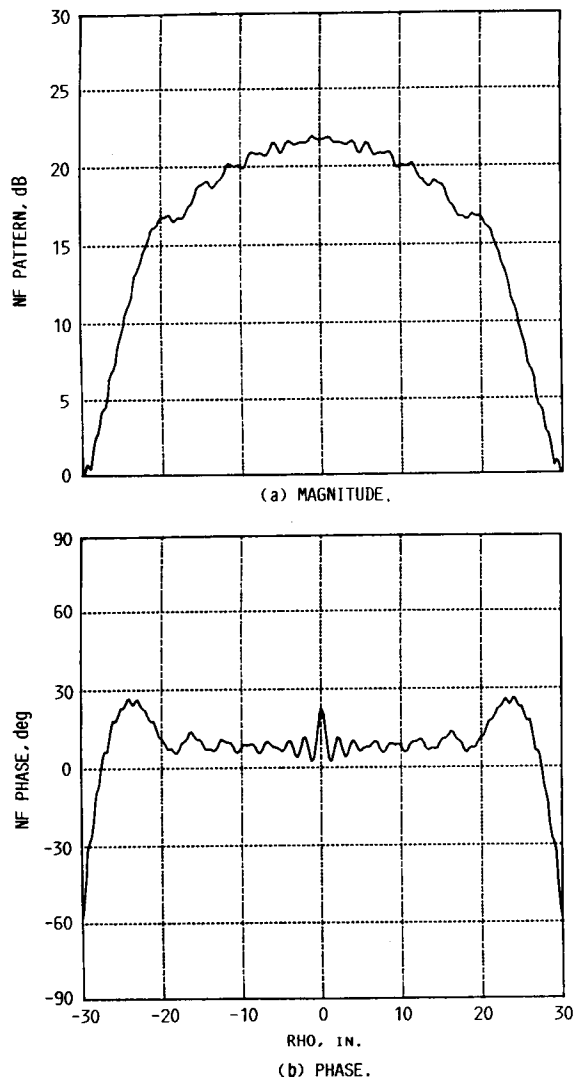


FIGURE 19. - HORIZONTAL SCAN OF THE NEAR FIELD AT  
 $z = 132$  IN. HALF SIZE ACCURATE ANTENNA REFLECTOR  
 WITH THE TRW DUAL MODE HORN. HORIZONTAL POLAR-  
 IZATION,  $f = 28.75$  GHZ.

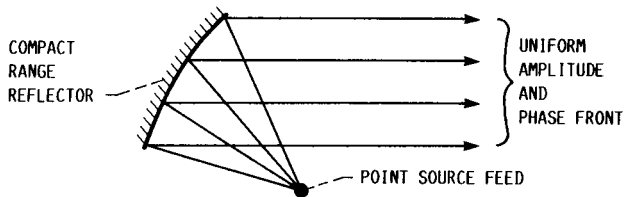


FIGURE 20. - "IDEAL" COMPACT RANGE.

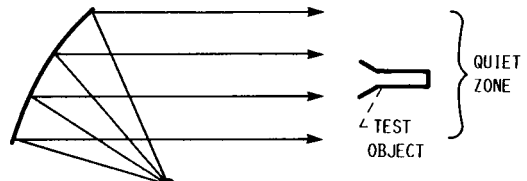


FIGURE 21. - MEASUREMENT IN THE "IDEAL" COMPACT RANGE.

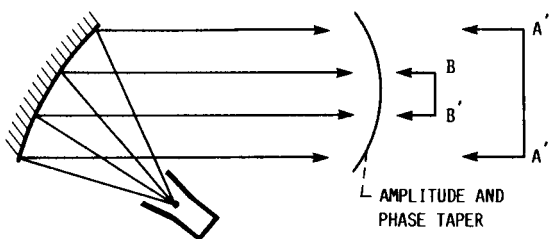


FIGURE 22. - AMPLITUDE AND PHASE TAPER IN THE QUIET ZONE DUE TO THE FEED PATTERN.

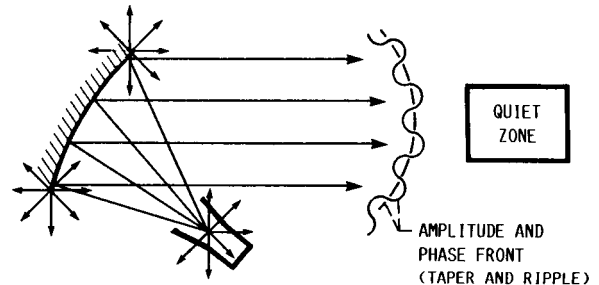


FIGURE 23. - AMPLITUDE AND PHASE RIPPLE FROM FEED SPOLOVER AND REFLECTOR EDGE DIFFRACTION.

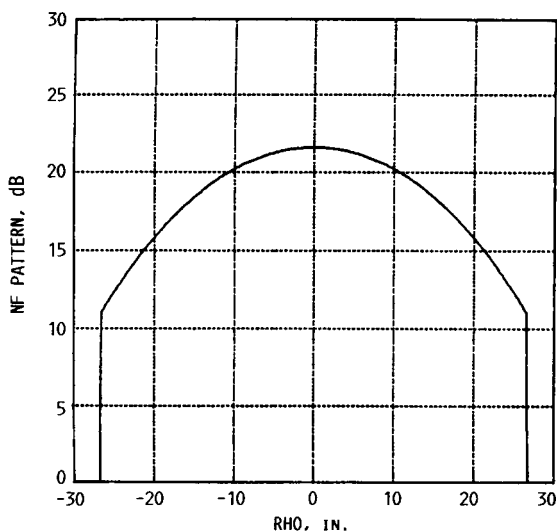


FIGURE 24. - MAGNITUDE OF THE G.O. FIELD IN THE HORIZONTAL PLANE OF THE HALF SCALE ACCURATE ANTENNA REFLECTOR WITH THE TRW DUAL MODE HORN FEED, HORIZONTAL POLARIZATION,  $f = 28.75$  GHz.

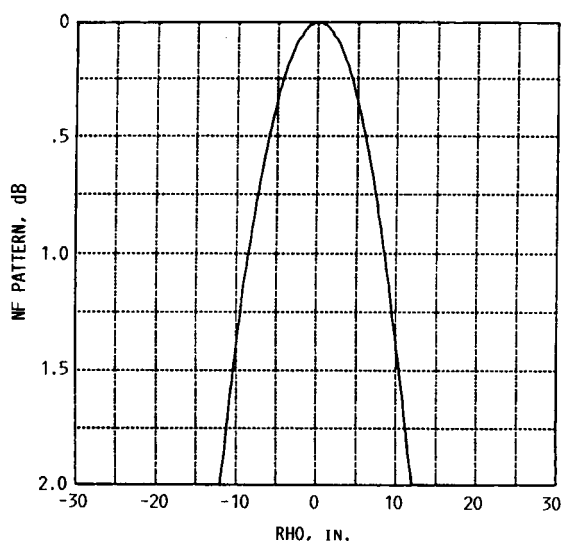


FIGURE 25. - MAGNITUDE OF THE G.O. FIELD IN THE HORIZONTAL PLANE OF THE HALF SCALE ACCURATE ANTENNA REFLECTOR WITH THE TRW DUAL MODE HORN FEED, HORIZONTAL POLARIZATION,  $f = 28.75$  GHz, EXPANDED SCALE.

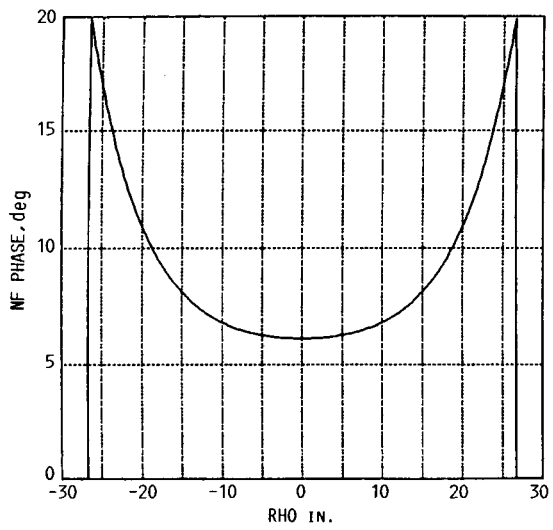


FIGURE 26. - PHASE OF THE G.O. FIELD IN THE HORIZONTAL PLANE OF THE HALF SCALE ACCURATE ANTENNA REFLECTOR WITH THE TRW DUAL MODE HORN FEED. HORIZONTAL POLARIZATION,  $f = 28.75$  GHz.

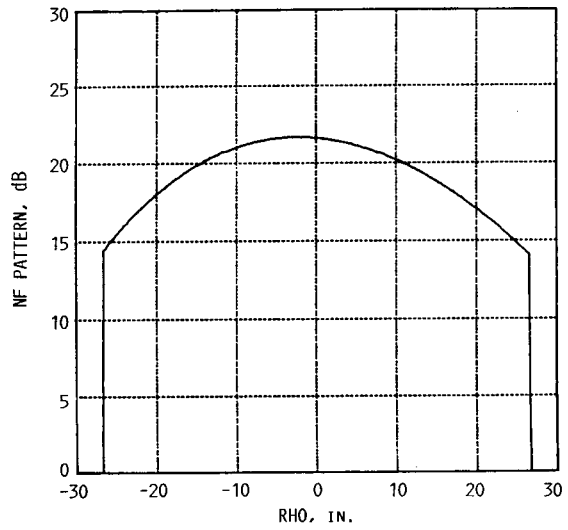


FIGURE 27. - MAGNITUDE OF THE G.O. FIELD IN THE VERTICAL PLANE OF THE HALF SCALE ACCURATE ANTENNA REFLECTOR WITH THE TRW DUAL MODE HORN FEED. HORIZONTAL POLARIZATION,  $f = 28.75$  GHz.

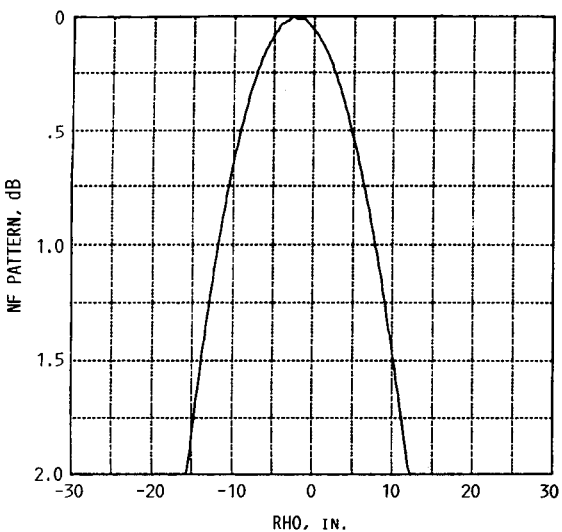


FIGURE 28. - MAGNITUDE OF THE G.O. FIELD IN THE VERTICAL PLANE OF THE HALF SCALE ACCURATE ANTENNA REFLECTOR WITH THE TRW DUAL MODE HORN FEED. HORIZONTAL POLARIZATION,  $f = 28.75$  GHz, EXPANDED SCALE.

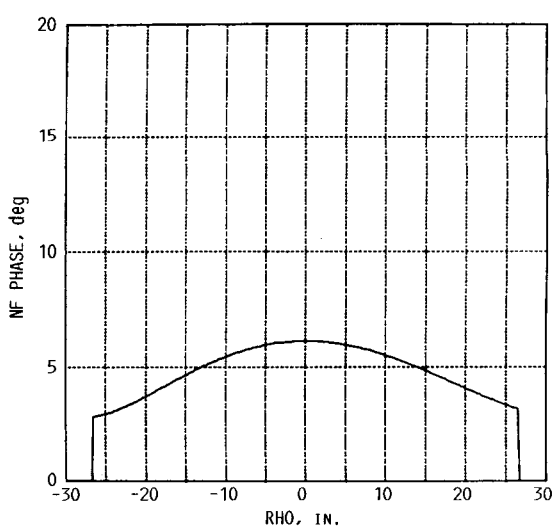


FIGURE 29. - PHASE OF THE G.O. FIELD IN THE VERTICAL PLANE OF THE HALF SCALE ACCURATE ANTENNA REFLECTOR WITH THE TRW DUAL MODE HORN FEED. HORIZONTAL POLARIZATION,  $f = 28.75$  GHz.

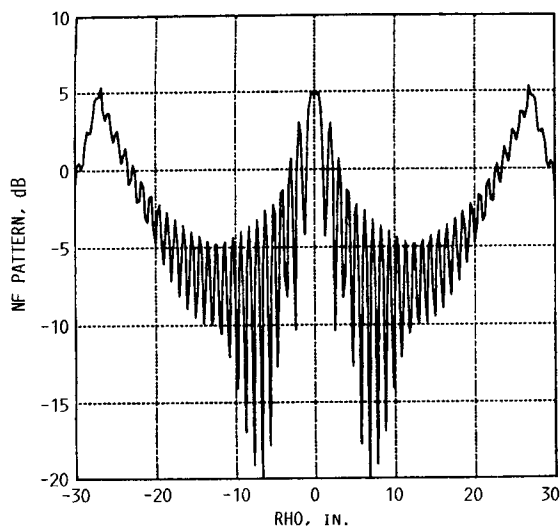


FIGURE 30. - MAGNITUDE OF THE DIFFRACTED FIELD IN THE HORIZONTAL PLANE OF THE HALF SCALE ACCURATE ANTENNA REFLECTOR WITH THE TRW DUAL MODE HORN FEED. HORIZONTAL POLARIZATION.  $f = 28.75$  GHz.

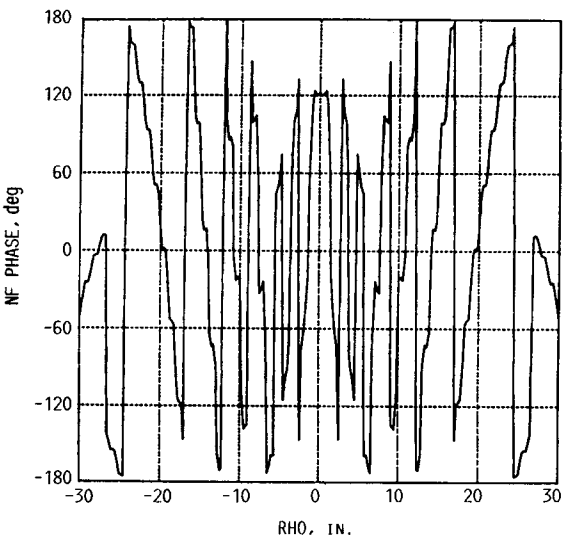


FIGURE 31. - PHASE OF THE DIFFRACTED IN THE HORIZONTAL PLANE OF THE HALF SCALE ACCURATE ANTENNA REFLECTION WITH THE TRW DUAL MODE HORN FEED. HORIZONTAL POLARIZATION.  $f = 28.75$  GHz.

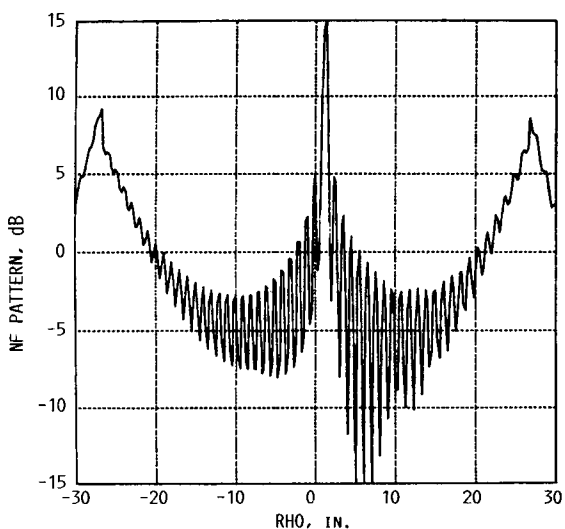


FIGURE 32. - MAGNITUDE OF THE DIFFRACTED FIELD IN THE VERTICAL FIELD PLANE OF THE HALF SCALE ACCURATE ANTENNA REFLECTOR WITH THE TRW DUAL MODE HORN FEED. HORIZONTAL POLARIZATION.  $f = 28.75$  GHz.

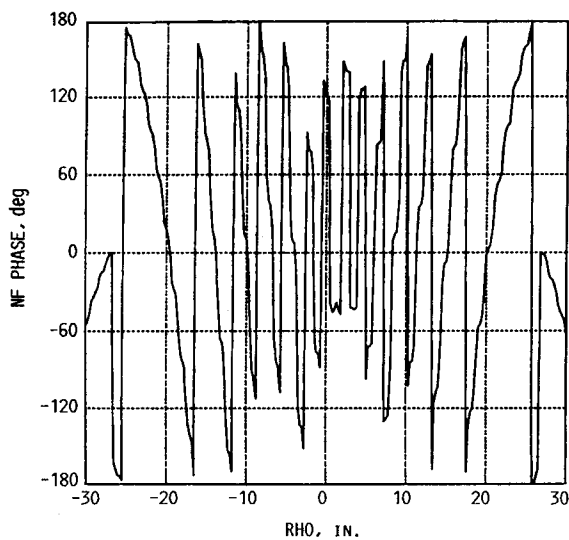


FIGURE 33. - PHASE OF THE DIFFRACTED FIELD IN THE VERTICAL PLANE OF THE HALF SCALE ACCURATE ANTENNA REFLECTOR WITH THE TRW DUAL MODE HORN FEED. HORIZONTAL POLARIZATION.  $f = 28.75$  GHz.

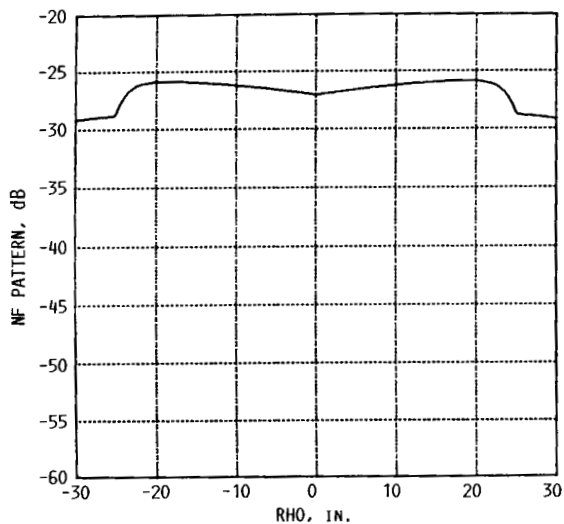


FIGURE 34. - MAGNITUDE OF THE FEED SPILLOVER IN THE HORIZONTAL PLANE OF THE HALF SCALE ACCURATE ANTENNA REFLECTOR WITH THE TRW DUAL MODE HORN FEED. HORIZONTAL POLARIZATION,  $f = 28.75$  GHz.

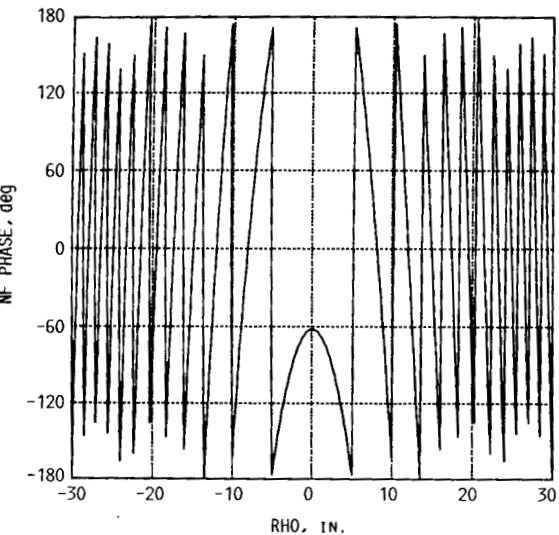


FIGURE 35. - PHASE OF THE FEED SPILLOVER IN THE HORIZONTAL PLANE OF THE HALF SCALE ACCURATE ANTENNA REFLECTOR WITH THE TRW DUAL MODE FEED. HORIZONTAL POLARIZATION,  $f = 28.75$  GHz.

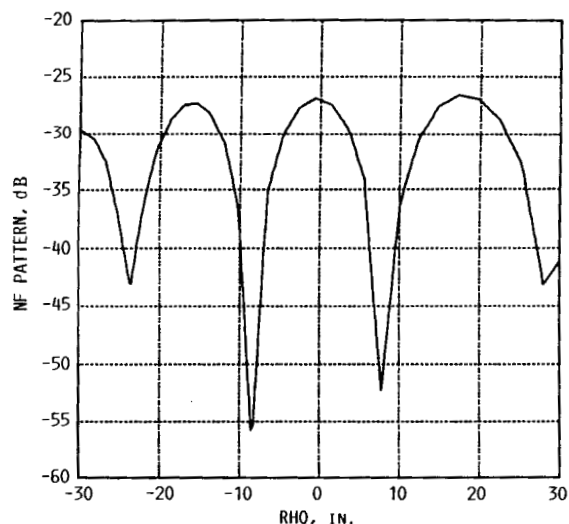


FIGURE 36. - MAGNITUDE OF THE SPILLOVER IN THE VERTICAL PLANE OF THE HALF SCALE ACCURATE ANTENNA REFLECTOR WITH THE TRW DUAL MODE HORN FEED. HORIZONTAL POLARIZATION,  $f = 28.75$  GHz.

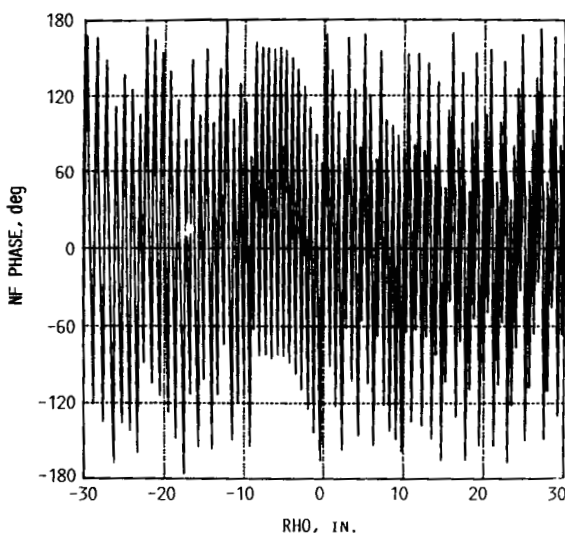


FIGURE 37. - PHASE OF THE FEED SPILLOVER IN THE VERTICAL PLANE OF THE HALF SCALE ACCURATE ANTENNA REFLECTOR WITH THE DUAL MODE HORN FEED. HORIZONTAL POLARIZATION,  $f = 28.75$  GHz.

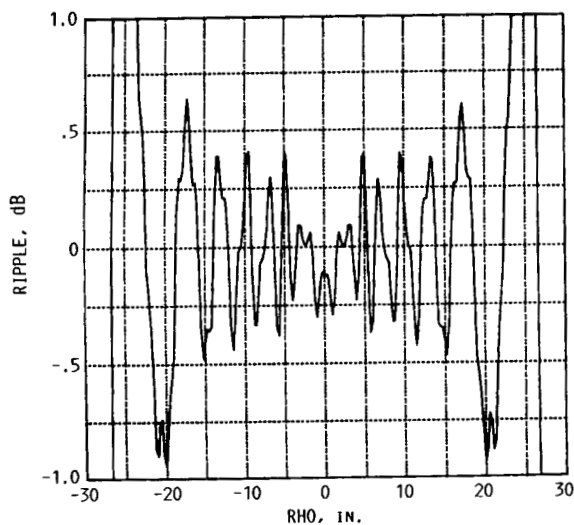


FIGURE 38. - RIPPLE IN THE HORIZONTAL PLANE OF THE HALF SCALE ACCURATE ANTENNA REFLECTOR WITH THE TRW DUAL MODE HORN FEED, HORIZONTAL POLARIZATION,  $f = 28.75$  GHz.

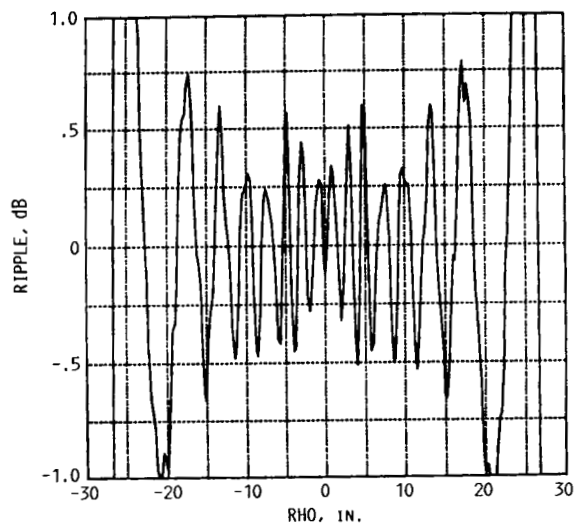


FIGURE 39. - RIPPLE IN THE VERTICAL PLANE OF THE HALF SCALE ACCURATE ANTENNA REFLECTOR WITH THE TRW DUAL MODE HORN FEED. HORIZONTAL POLARIZATION,  $f = 28.75$  GHz.

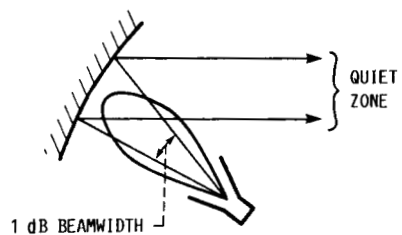


FIGURE 40. - QUIET ZONE RELATIONSHIP TO FEED PATTERN.

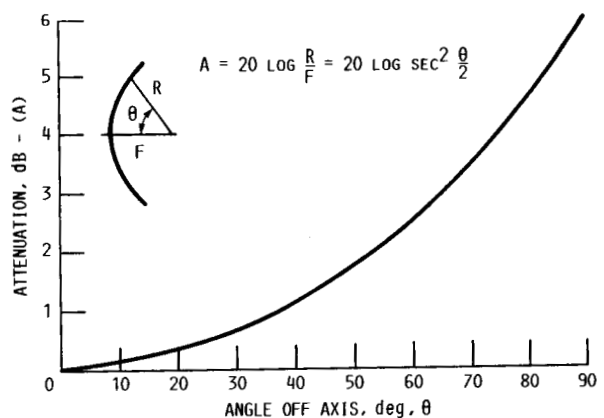


FIGURE 41. - SPACE ATTENUATION VERSUS FEED ANGLE.

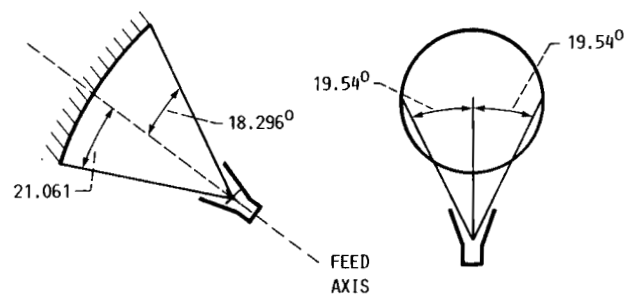


FIGURE 42. - LOCATION OF REFLECTOR EDGE IN FEED PATTERN COORDINATES.

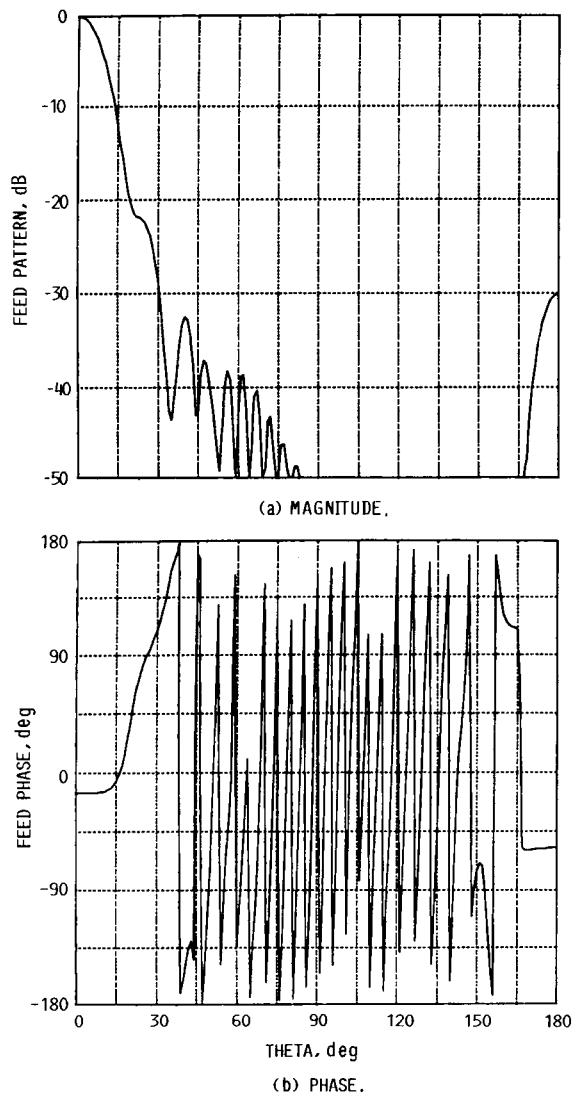


FIGURE 43. - CORRUGATED HORN FEED PATTERN WHICH WILL PROVIDE A -20 dB EDGE TAPER.

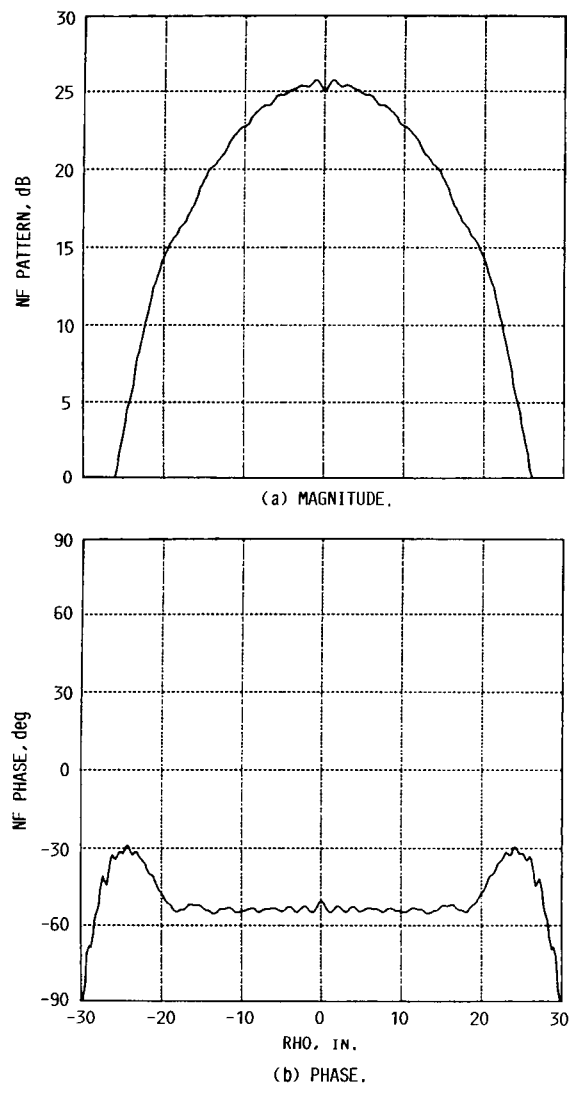
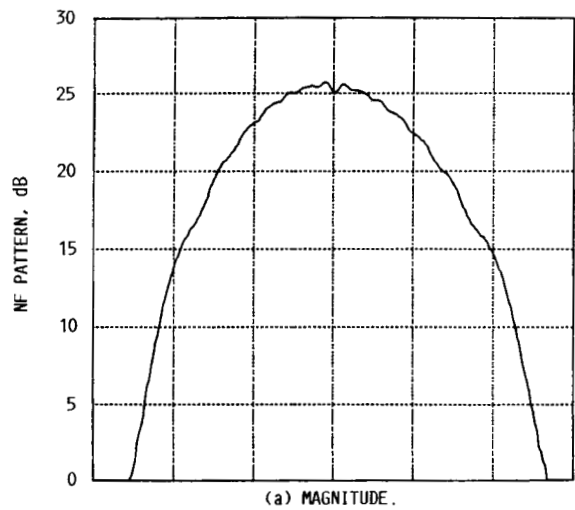
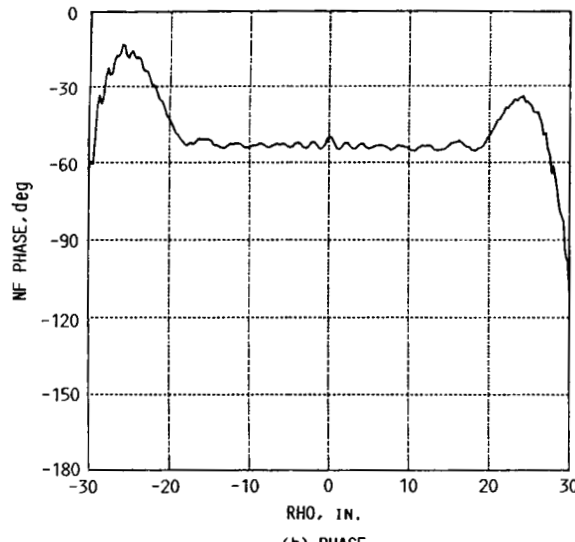


FIGURE 44. - HORIZONTAL SCAN OF THE NEAR FIELD AT  $Z = 132$  IN. HALF SIZE ACCURATE ANTENNA REFLECTOR WITH THE -20 dB EDGE ILLUMINATION. HORIZONTAL POLARIZATION,  $f = 28.75$  GHz.



(a) MAGNITUDE.



(b) PHASE.

FIGURE 45. - VERTICAL SCAN OF THE FIELD AT  $z = 132$  IN.  
HALF SIZE ACCURATE ANTENNA REFLECTOR WITH THE -20 dB  
EDGE ILLUMINATION. HORIZONTAL POLARIZATION,  $f = 28.75$   
GHz.

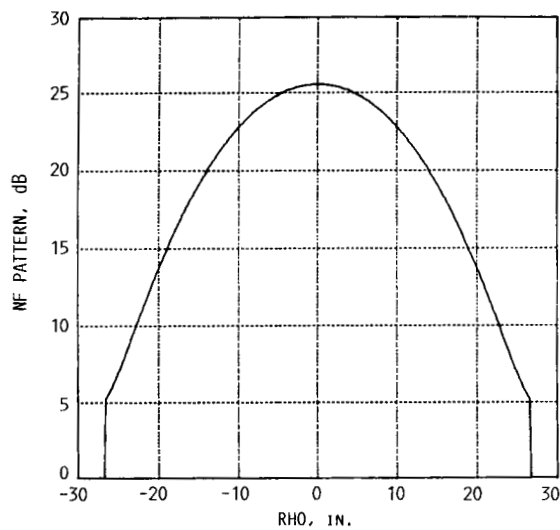


FIGURE 46. - MAGNITUDE OF THE G.O. FIELD IN THE HORIZONTAL PLANE OF THE HALF SCALE ACCURATE ANTENNA REFLECTOR WITH THE -20 dB EDGE ILLUMINATION. HORIZONTAL POLARIZATION,  $f = 28.75$  GHz.

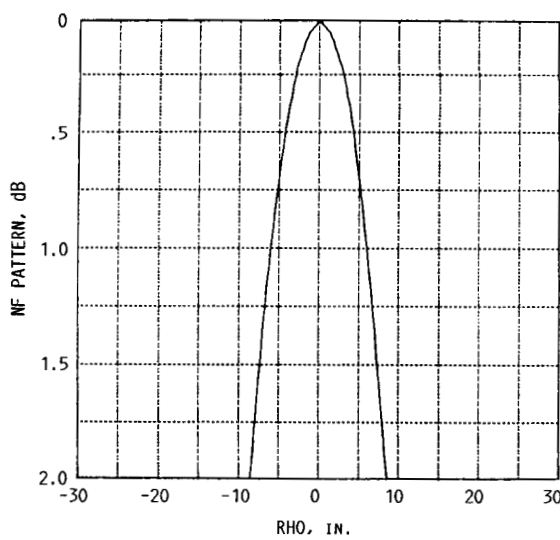


FIGURE 47. - MAGNITUDE OF THE G.O. FIELD IN THE HORIZONTAL PLANE OF THE HALF SCALE ACCURATE ANTENNA REFLECTOR WITH THE -20 dB EDGE ILLUMINATION. HORIZONTAL POLARIZATION,  $f = 28.75$  GHz, EXPANDED SCALE.

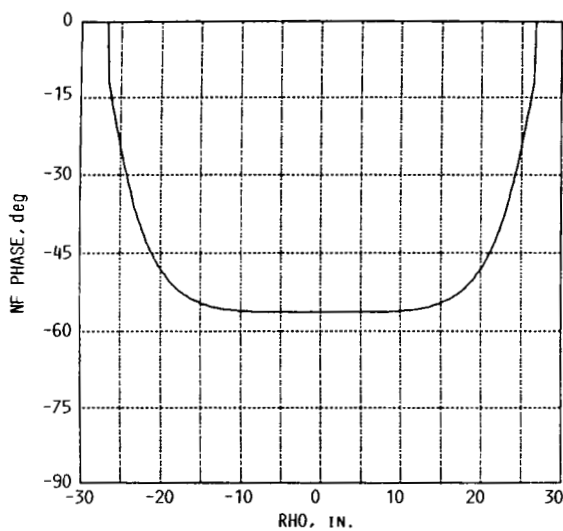


FIGURE 48. - PHASE OF THE G.O. FIELD IN THE HORIZONTAL PLANE OF THE HALF SCALE ACCURATE ANTENNA REFLECTOR WITH THE -20 dB EDGE ILLUMINATION HORIZONTAL POLARIZATION,  $f = 28.75$  GHz.

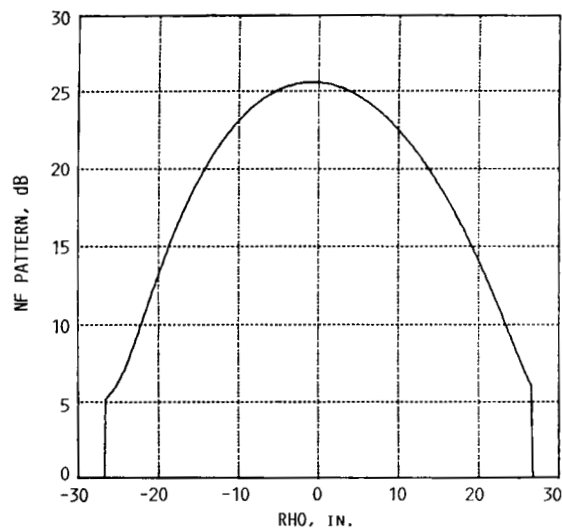


FIGURE 49. - MAGNITUDE OF THE G.O. FIELD IN THE VERTICAL PLANE OF THE HALF SCALE ACCURATE ANTENNA REFLECTOR WITH THE -20 dB EDGE ILLUMINATION, HORIZONTAL POLARIZATION,  $f = 28.75$  GHz.

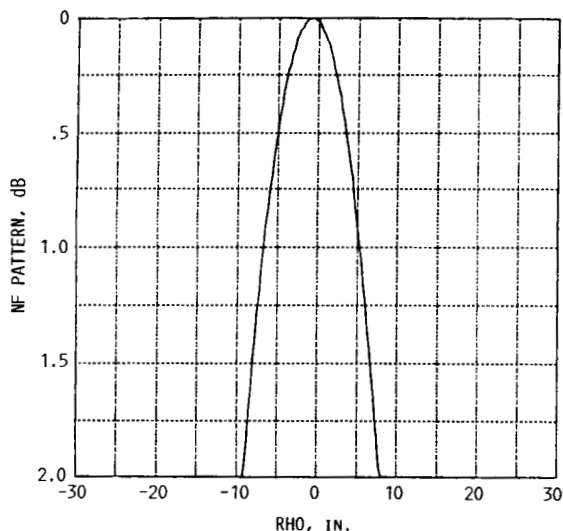


FIGURE 50. - MAGNITUDE OF THE G.O. FIELD IN THE VERTICAL PLANE OF THE HALF SCALE ACCURATE ANTENNA REFLECTOR WITH THE -20 dB EDGE ILLUMINATION, HORIZONTAL POLARIZATION,  $f = 28.75$  GHz, EXPANDED SCALE.

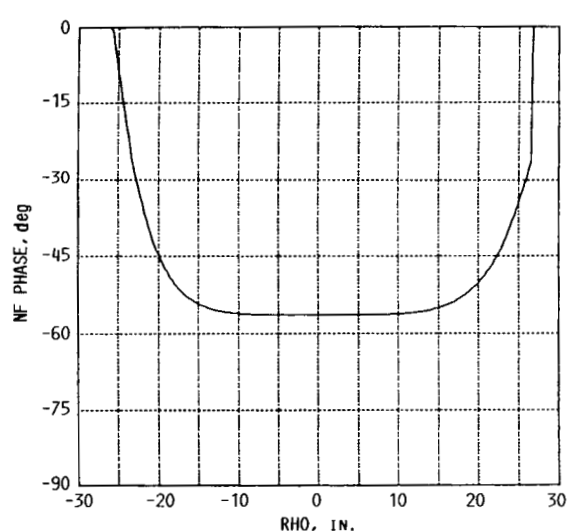


FIGURE 51. - PHASE OF THE G.O. FIELD IN THE VERTICAL PLANE OF THE HALF SCALE ACCURATE ANTENNA REFLECTOR WITH THE -20 dB EDGE ILLUMINATION, HORIZONTAL POLARIZATION,  $f = 28.75$  GHz.

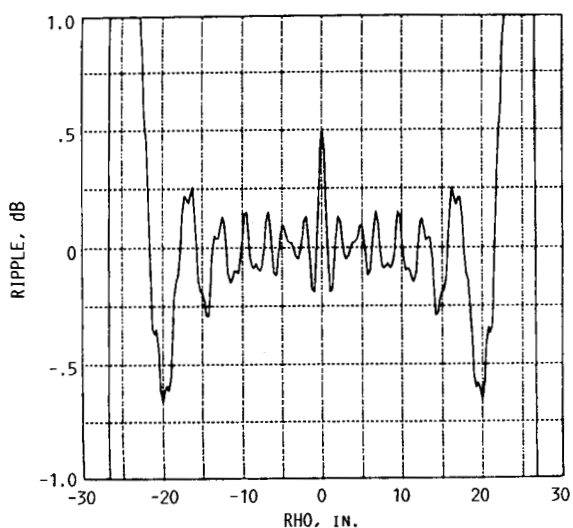


FIGURE 52. - RIPPLE IN THE HORIZONTAL PLANE OF THE HALF SCALE ACCURATE ANTENNA REFLECTOR WITH THE -20 dB EDGE ILLUMINATION. HORIZONTAL POLARIZATION,  $f = 28.75$  GHZ.

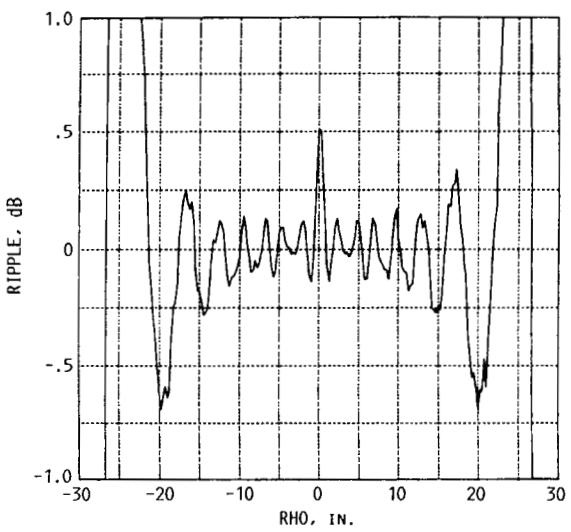


FIGURE 53. - RIPPLE IN THE VERTICAL PLANE OF THE HALF SCALE ACCURATE ANTENNA REFLECTOR WITH THE -20 dB EDGE ILLUMINATION. HORIZONTAL POLARIZATION,  $f = 28.75$  GHZ.

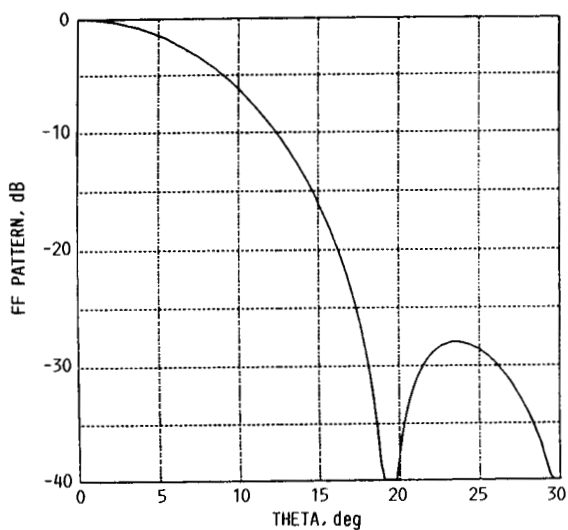


FIGURE 54. - CORRUGATED WAVEGUIDE FEED PATTERN WHICH WILL PRODUCE A -30 dB EDGE TAPER.

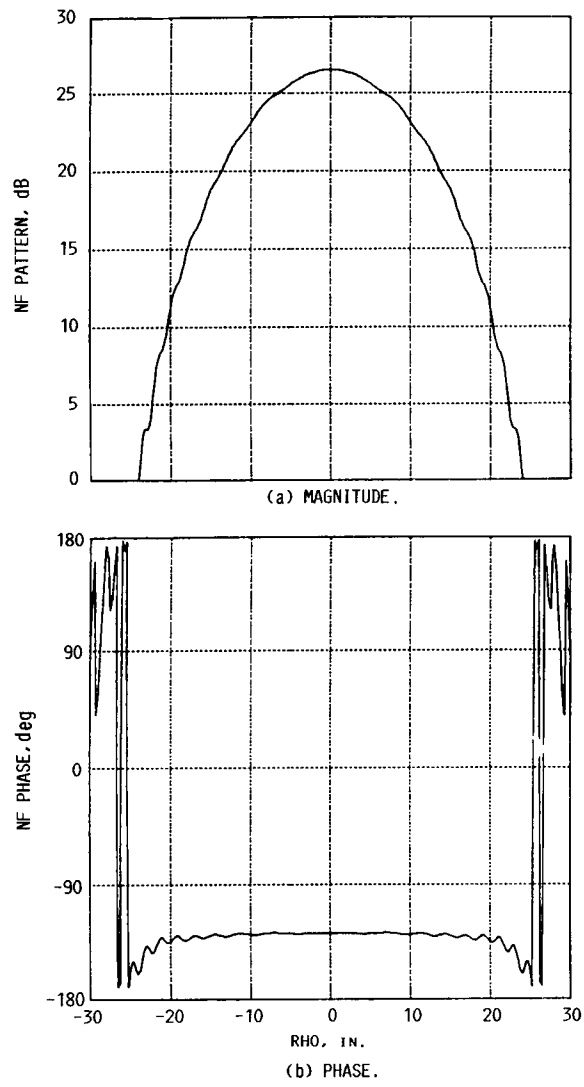


FIGURE 55. - HORIZONTAL SCAN OF THE NEAR FIELD AT  
z = 132 IN. HALF SIZE ACCURATE ANTENNA REFLECTOR  
WITH THE -30 dB EDGE ILLUMINATION. HORIZONTAL  
POLARIZATION, f = 28.75 GHz.

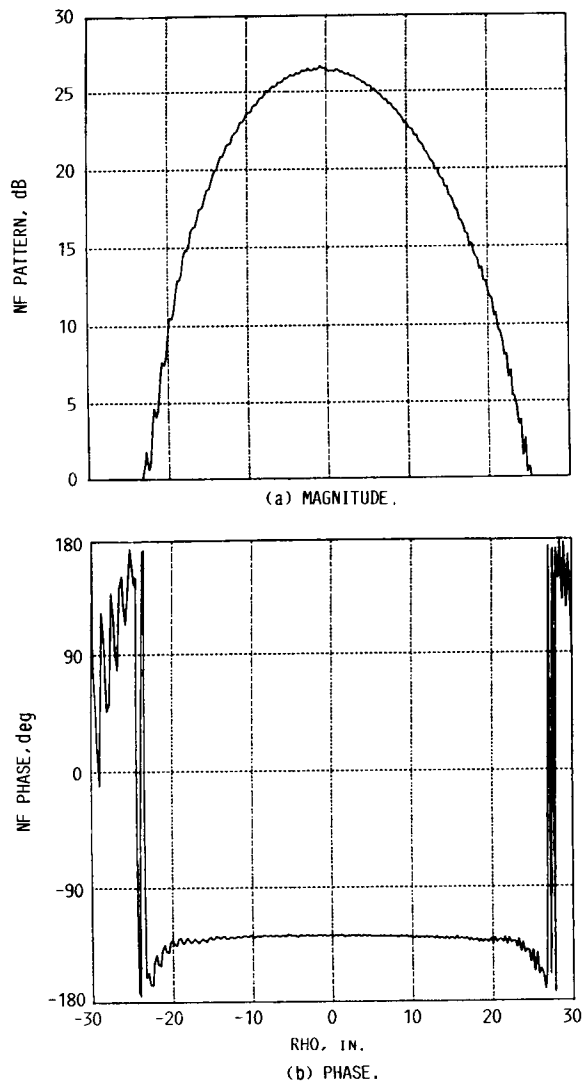


FIGURE 56. - VERTICAL SCAN OF THE FIELD AT z = 132 IN.  
HALF SIZE ACCURATE ANTENNA REFLECTOR WITH THE -30 dB  
EDGE ILLUMINATION. HORIZONTAL POLARIZATION, f = 28.75  
GHz.

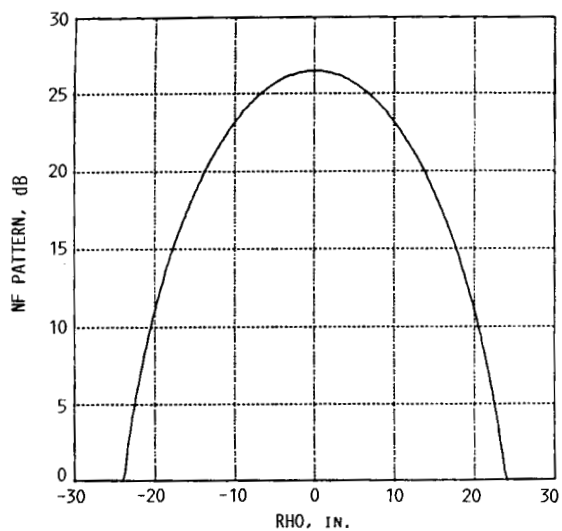


FIGURE 57. - MAGNITUDE OF THE G.O. FIELD IN THE HORIZONTAL PLANE OF THE HALF SCALE ACCURATE ANTENNA REFLECTOR WITH THE -30 dB EDGE ILLUMINATION, HORIZONTAL POLARIZATION,  $f = 28.75$  GHz.

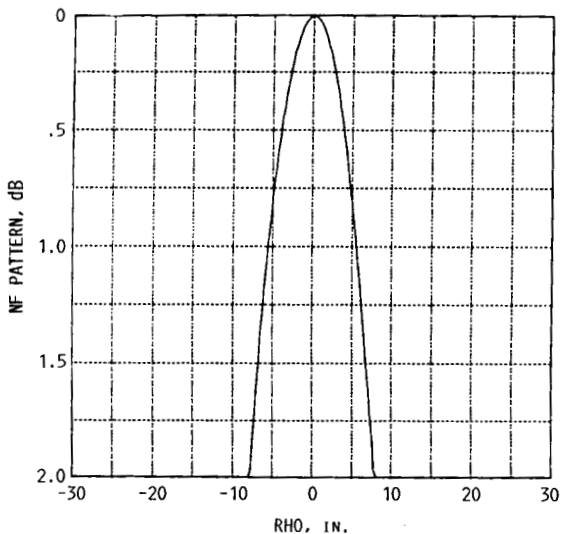


FIGURE 58. - MAGNITUDE OF THE G.O. FIELD IN THE HORIZONTAL PLANE OF THE HALF SCALE ACCURATE ANTENNA REFLECTOR WITH THE -30 dB EDGE ILLUMINATION, HORIZONTAL POLARIZATION,  $f = 28.75$  GHz, EXPANDED SCALE.

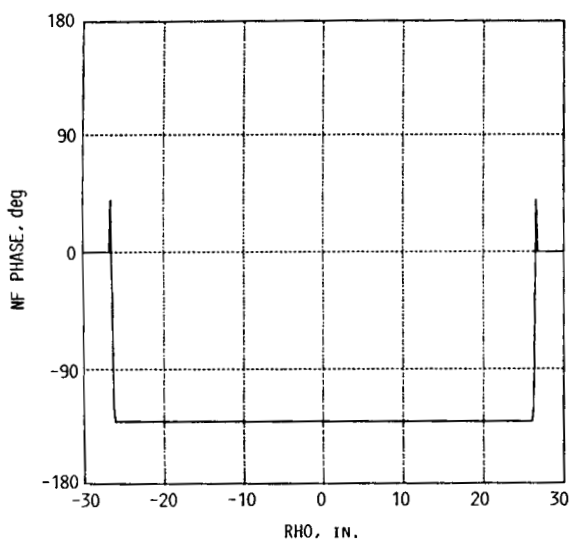


FIGURE 59. - PHASE OF THE G.O. FIELD IN THE HORIZONTAL PLANE OF THE HALF SCALE ACCURATE ANTENNA REFLECTOR WITH THE -30 dB EDGE ILLUMINATION, HORIZONTAL POLARIZATION,  $f = 28.75$  GHz.

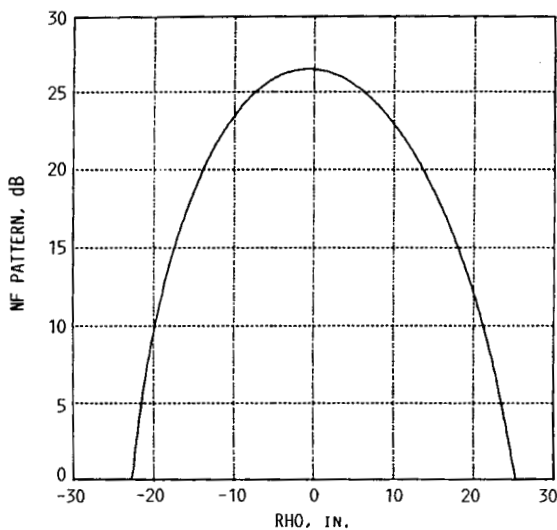


FIGURE 60. - MAGNITUDE OF THE G.O. FIELD IN THE VERTICAL PLANE OF THE HALF SCALE ACCURATE ANTENNA REFLECTOR WITH THE -30 dB EDGE ILLUMINATION, HORIZONTAL POLARIZATION,  $f = 28.75$  GHz.

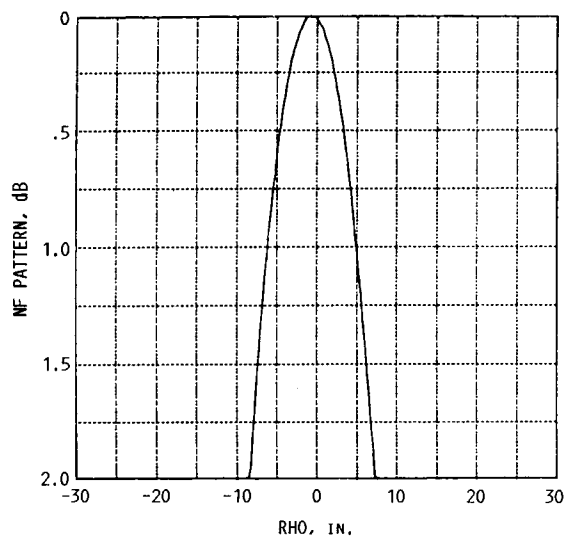


FIGURE 61. - MAGNITUDE OF THE HALF SCALE ACCURATE ANTENNA REFLECTOR WITH THE -30 dB EDGE ILLUMINATION, HORIZONTAL POLARIZATION,  $f = 28.75$  GHz, EXPANDED SCALE.

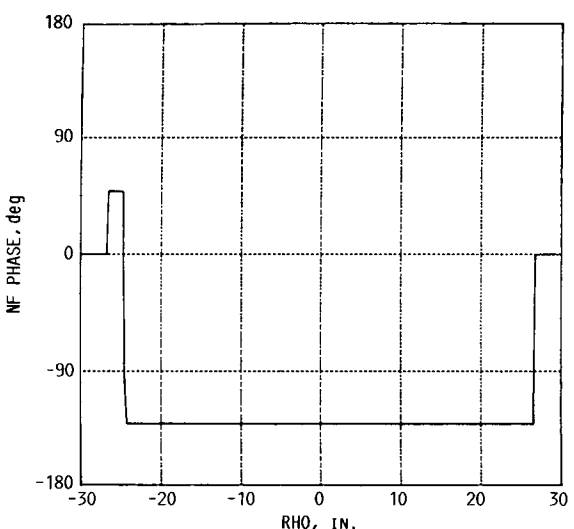


FIGURE 62. - PHASE OF THE G.O. FIELD IN THE VERTICAL PLANE OF THE HALF SCALE ACCURATE ANTENNA REFLECTOR WITH THE -30 dB EDGE ILLUMINATION,  $f = 28.75$  GHz.

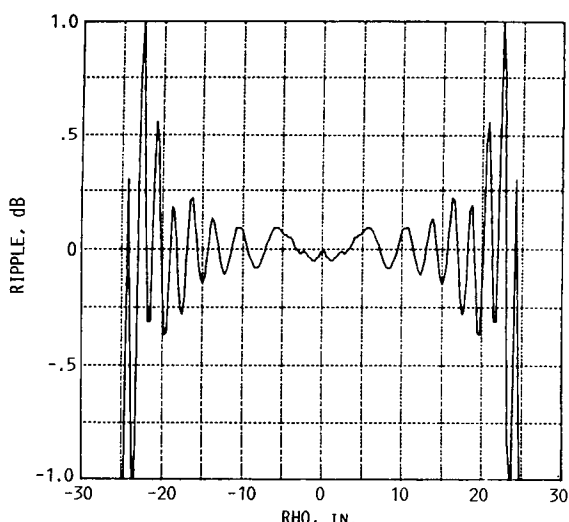


FIGURE 63. - RIPPLE IN THE HORIZONTAL PLANE OF THE HALF SCALE ACCURATE ANTENNA REFLECTOR WITH THE -30 dB EDGE ILLUMINATION, HORIZONTAL POLARIZATION,  $f = 28.75$  GHz.

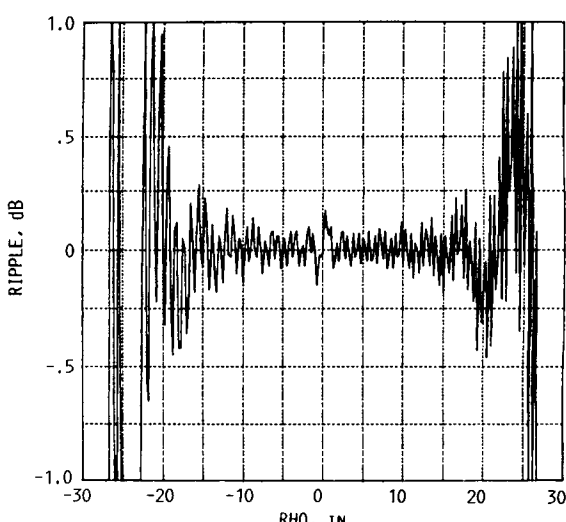


FIGURE 64. - RIPPLE IN THE VERTICAL PLANE OF THE HALF SCALE ACCURATE ANTENNA REFLECTOR WITH THE -30 dB EDGE ILLUMINATION, HORIZONTAL POLARIZATION,  $f = 28.75$  GHz.



National Aeronautics and  
Space Administration

## Report Documentation Page

1. Report No.  NASA CR-182284	2. Government Accession No.	3. Recipient's Catalog No.	
4. Title and Subtitle  Computed Performance of the Half-Scale Accurate Antenna Reflector		5. Report Date  May 1989	
		6. Performing Organization Code	
7. Author(s)  Kevin M. Lambert	8. Performing Organization Report No.  None (E-4748)		
9. Performing Organization Name and Address  Analex Corporation NASA Lewis Research Center Cleveland, Ohio 44135		10. Work Unit No.  506-44-2A	
12. Sponsoring Agency Name and Address  National Aeronautics and Space Administration Lewis Research Center Cleveland, Ohio 44135-3191		11. Contract or Grant No.	
13. Type of Report and Period Covered  Contractor Report Final			
14. Sponsoring Agency Code			
15. Supplementary Notes  Project Manager, Charles A. Raquet, Space Electronics Division, NASA Lewis Research Center.			
16. Abstract  This report studies the performance of the half-scale, accurate antenna reflector. The antenna is evaluated for use as a compact range reflector. The reflector is studied for use with three separate feed antennas.			
17. Key Words (Suggested by Author(s))  Reflector antennas Compact ranges		18. Distribution Statement  Unclassified - Unlimited Subject Category 33	
19. Security Classif. (of this report)  Unclassified	20. Security Classif. (of this page)  Unclassified	21. No of pages  32	22. Price*  A03